Nucleophilic substitution by amide nitrogen in the aromatic rings of $[z_n - H]^{\bullet+}$ ions; the structures of the $[b_2 - H - 17]^{\bullet+}$ and $[c_1 - 17]^{+}$ ions

Xiaoyan Mu,[a] Justin Kai-Chi Lau,[b,c] Cheuk-Kuen Lai,[a] K.W. Michael Siu,[b,c] Alan C. Hopkinson,[b] Ivan K. Chu[a*]*

[a]*Department of Chemistry, The University of Hong Kong, Hong Kong, China*
[b]*Department of Chemistry and Centre for Research in Mass Spectrometry, York University, 4700 Keele Street, Toronto ON, Canada M3J 1P3*
[c]*Department of Chemistry and Biochemistry, University of Windsor, 401 Sunset Avenue, Windsor, ON, Canada N9B 3P4*

*Corresponding authors

Email: ach@yorku.ca; ivankchu@hku.hk

Abstract

Peptide radical cations that contain an aromatic amino acid residue cleave to give $[z_n - H]^{\bullet+}$ ions with $[b_2 - H - 17]^{\bullet+}$ and $[c_1 - 17]^{+}$ ions, the dominant products in the dissociation of $[z_n - H]^{\bullet+}$, also present in lower abundance in the CID spectra. Isotopic labeling in the aromatic ring of $[Y_{\pi}^{\bullet}GG]^{+}$ establishes that in the formation of $[b_2 - H - 17]^{\bullet+}$ ions a hydrogen from the δ-position of the Y residue is lost, indicating that nucleophilic substitution on the aromatic ring has occurred. A preliminary DFT investigation of nine plausible structures for the $[c_1 - 17]^{+}$ ion derived from $[Y_{\pi}^{\bullet}GG]^{+}$ shows that two structures resulting from attack on the aromatic ring by oxygen and nitrogen atoms from the peptide backbone have significantly better energies than other isomers. A detailed study of $[Y_{\pi}^{\bullet}GG]^{+}$ using two density functionals, B3LYP and M06-2X, with a 6-31++G(d,p) basis set gives a higher barrier for attack on the aromatic ring of the $[z_n - H]^{\bullet+}$ ion by nitrogen than by the carbonyl oxygen. However, subsequent rearrangements involving proton transfers are much higher in energy for the oxygen-substituted isomer leading to the conclusion that the $[c_1 - 17]^{+}$ ions are the products of nucleophilic attack by nitrogen, protonated 2,7-dihydroxyquinoline ions. The $[b_2 - H - 17]^{\bullet+}$ ions are formed by loss of glycine from the same intermediates involved in the formation of the $[c_1 - 17]^{+}$ ions.

Keywords: collision-induced dissociation, peptide radical cations, fragmentation mechanism, density functional theory, backbone-aromatic ring bond.

Introduction

Gas-phase fragmentation of peptides is a key technology for peptide sequencing and, ultimately, protein identification with the use of biological mass spectrometry.[1-3] The gas-phase fragmentations of even-electron peptides of the type $[M + nH]^{n+}$ have been studied extensively and interpreted with the aid of the 'mobile proton model'.[4-10] Low-energy collision-induced dissociation (CID) initiates charge-directed cleavages at different amide bonds along the peptide backbone, forming *b*- or *y*- ions, typically through a series of proton transfers and subsequent intramolecular nucleophilic attack. Hydrogen-deficient peptide radical cations undergo many of the same type of charge-driven cleavages but there are also diverse radical-induced dissociation pathways that differ substantially from those of their protonated counterparts and those of hydrogen-rich peptide radical cations, thereby providing much additional information for protein and peptide sequencing.[11-19] Recent investigations have indicated that cationic peptide radicals undergo both backbone and side-chain cleavages.[18, 20-25] Among the backbone cleavages, N–C_α,[26-29] N-terminal amide,[30-32] and C_α–C bond cleavages,[33-35] which produce $[c_n + 2H]^+/[z_n - H]^{\bullet+}$ ions, $[y_{n-1}]^+$ ions, and $[a_n]^+/[z_n + H]^{\bullet+}$ ions, respectively, have been observed; known side-chain reactions include C_α–C_β and C_β–C_γ bond cleavages.[30-32, 35-38] The nomenclature used for describing product ions is the recently proposed 'all-explicit' system.[39]

Peptide and protein radicals are common features of cellular metabolism.[40-42] The presence of free radicals can lead to protein damage that results in various diseases, ranging from atherosclerosis and myocardial infarction to cancer and aging.[43-47] On the positive side, free radicals are responsible for protein activity and degradation, cytolysis and cell functioning.[40, 42, 48] Fragmentations of phenylalanine-, tyrosine- and tryptophan-containing peptide radical cations have attracted significant attention since these aromatic amino acids have interesting properties and are found in numerous proteins. One of their functions is in the transport of electrons or electron holes over long distances in proteins by virtue of their easily oxidized side chains.[49-51]

Free radical attack may also cause protein fragmentation and protein conformational changes, both of which can alter the protein function significantly.[46, 47]

Knowledge about how specific residues can induce unusual modes of fragmentation can assist in identification of peptides. Formation of $[z_n - H]^{\bullet+}$ ions by cleavage of the N–C_α bond of an aromatic acid residue is a common pathway in the dissociation of peptide radical cations and the existence of these ions helps in determining the location of the aromatic amino acid.[27-29] Here we report that dissociation of the $[z_n - H]^{\bullet+}$ ions results in the formation of residue-specific product ions at *m/z* 146 and 187 for phenylalanine-, 162 and 203 for tyrosine-, and 185 and 226 for tryptophan- containing peptides. The ion with the lower mass-to-charge within each category is a $[c_1 - 17]^+$ ion and the one with the higher mass-to-charge is a $[b_2 - H - 17]^{\bullet+}$ ion. The observation of these product ions, along with the *m/z* value of the $[z_n - H]^{\bullet+}$ ion, reveals the presence and the position of phenylalanine, tyrosine, tryptophan residues in a peptide chain. Here detailed mechanisms are examined using the tripeptide radical cation $[Y_\pi^{\bullet}GG]^+$ as a model to rationalize how these diagnostic fragment ions are formed. Loss of an aromatic hydrogen shows that the $[b_2 - H - 17]^{\bullet+}$ ions are the products of a novel interaction between the backbone of the peptide and the aromatic side chain. Density functional theory establishes that both product ions are the results of attack by the amide nitrogen on the aromatic ring.

Experimental section

Materials and Reagents

Fmoc-protected amino acids and Wang resin were purchased from Advanced ChemTech (Louisville, KY, USA). All of the studied peptides were synthesized according to procedures described in the literature.[52] All solvents were of HPLC grade; menthol, water, and acetic acid were purchased from Duksan Pure Chemicals (Ansan-City, Gyungkido, Korea), Tedia (Fairfield, OH, USA), and VWR International (Poole, England), respectively. Copper(II)-containing ternary

complexes were prepared by mixing copper(II) perchlorate hexahydrate with the crown ether either 1,4,7,10-tetraoxacyclododecane (12-crown-4) or 1,4,7,10,13,16-hexaoxacyclooctadecane (18-crown-6) in a water/methanol solution (1:1).

Mass Spectrometry

Experiments were carried out on a triple quadrupole linear-ion trap (LIT) (QTRAP®, AB SCIEX, Concord, ON, Canada) equipped with an electrospray ionization (ESI) source and nitrogen as the curtain and collision gas. In a typical infusion experiment, a syringe pump (Cole Parmer, Vernon Hills, IL, USA) was used to deliver samples at a flow rate of 180 μL h^{-1}. The peptide stock solutions for experiments with singly protonated peptides typically comprised 0.1 mM peptide in H_2O/MeOH (50:50, v/v) containing 0.1% AcOH. When generating peptide radicals using metal complexes, 600 μM Cu^{II}(12-crown-4)$(NO_3)_2$ or Cu^{II}(18-crown-6)$(NO_3)_2$ was added to the peptide stock solutions, without AcOH, such that peptide radical ions ($M^{\bullet+}$) would be generated through one-electron transfer from the neutral peptide to the metal center in the metal–ligand–peptide ternary complex. The specific α-carbon-centered radicals were formed through multistage CID of $[Cu^{II}(ligand)(M)]^{\bullet 2+}$, in which peptide canonical radical cations $M^{\bullet+}$ were generated in the first stage of CID of metal-ligand-peptide complexes and then underwent a subsequent stage of CID to generate the α-carbon-centered radical through side-chain loss.

Computational Methods

Structures of the π-radical $[Y_\pi^{\bullet}GG]^+$ and its dissociation products were initially obtained through Monte Carlo conformational searches with a semi-empirical method (PM3) using the Spartan software.[53] This was followed by geometry optimizations in the framework of density functional theory (DFT) using the unrestricted (U) hybrid functional formulated with a mixture of Hartree–Fock exchange energy and Becke's three-parameter 1988 gradient-corrected exchange energy, as well as Lee–Yang–Parr (LYP) correlation energy (UB3LYP).[54, 55] All DFT calculations

were performed initially with the 6-31G(d) basis set and subsequently with the 6-31++G(d,p) basis set[56, 57], i.e. at the UB3LYP/6-31++G(d,p) levels. All of the stationary points were characterized by vibrational analysis to ensure that their curvatures were correct on the corresponding potential energy surfaces (PESs); the intrinsic reaction coordinate (IRC) method[58] was used to identify the local minima associated with each transition structure. Relative enthalpies at 0 K ($\Delta H_0°$) were calculated from the electronic energies and zero-point energies (ZPVE) obtained within the harmonic approximation. Subsequently, all the structures at critical points were re-optimized using the M06-2X functional and, as there are significant differences, both sets of data are reported.[59, 60] All DFT calculations were performed using the Gaussian 09 software package.[61]

Results and Discussion

The discovery of residue-specific product ions

The CID spectrum of the canonical radical cation tyrosylglycylglycylglycine $[Y_{\pi}^{\bullet}GGG]^+$ in which the charge and spin are delocalized in the π-system of the tyrosine side chain is shown in Figure 1a. The dominant fragmentation pathway is loss of the tyrosine side chain as *p*-quinomethide (-106 Da) by radical-induced C_α–C_β bond cleavage; a second channel, ammonia loss (-17 Da) by cleaving the N-terminal N–C_α bond to give the $[z_4 - H]^{\bullet+}$ ion, is moderately abundant. Products in lower abundance are the $[b_2 - H]^{\bullet+}$ ion (at *m/z* 220), the product of charge-induced dissociation of the second amide bond, the $[b_2 - H - 17]^{\bullet+}$ ion (at *m/z* 203), and a more unusual product ion, the $[c_1 - 17]^+$ ion at *m/z* 162. The CID spectrum of an alanine-containing analogous peptide $[YGGA]^{\bullet+}$ (i.e., replacing the C-terminal glycine residue by an alanine residue, Figure S1a in supplementary materials), establishes that all these minor product ions contain remnants of the N-terminal tyrosine residue. The $[b_2 - H - 17]^{\bullet+}$ and $[c_1 - 17]^+$ ions are the major dissociation products of the $[z_4 - H]^{\bullet+}$ ion, as shown in Figure 1b and Figure S1b; similar results are also observed in the CID spectrum of the tripeptide

tyrosylglycylglycine $[Y_{\pi}^{\bullet}GG]^+$ (Figure S2). These observations provide experimental evidence that formation of these two residue-specific product ions are probably formed via the intermediacy of the $[z_n - H]^{\bullet+}$ product ion. Surprisingly, the CID spectrum of the $[c_1 - 17]^+$ ion reveals the elimination of a water molecule (Figure 1c) and, at first glance, it is not readily apparent what structural features facilitate this loss. These observations, when coupled with the fact that isotopic labeling established that one of the aromatic hydrogen is lost in forming the $[b_2 - H - 17]^{\bullet+}$ ion *vide infra,* indicates that structural rearrangement involving attack on the aromatic ring by a nucleophile from the backbone occurs.

The N–C_{α} bonds of other aromatic amino acid residues in peptide radical cations are also susceptible to heterolytic cleavage yielding $[z_n - H]^{\bullet+}$ ions. This is illustrated in Figure 2a and 2c for $[W_{\pi}^{\bullet}GG]^+$ and $[FGG_{\alpha}^{\bullet}]^+$ (radical at the α-carbon of the C-terminal residue). Many additional examples are available in the Supplemental Materials. In these spectra, the $[c_1 - 17]^+$ and $[b_2 - H - 17]^{\bullet+}$ ions are ubiquitous, although sometimes in low abundance. CID spectra of the $[z_3 - H]^{\bullet+}$ fragment ions generated from $[W_{\pi}^{\bullet}GG]^+$ and $[FGG_{\alpha}^{\bullet}]^+$ (Figures 2b and 2d) produce the fragment ions $[c_1 - 17]^+$ at *m/z* 185 and 146, and $[b_2 - H - 17]^{\bullet+}$ at *m/z* 226 and 187, respectively. As observed for $[Y_{\pi}^{\bullet}GGG]^+$, the $[c_1 - 17]^+$ ions of $[W_{\pi}^{\bullet}GG]^+$ and $[F_{\pi}^{\bullet}GG]^+$ both dissociated by loss of water (Figures S3a and Figures S4c). By contrast, the $[b_2 - H - 17]^{\bullet+}$ ion appears to be quite fragile and easily loses a hydrogen atom, as observed in the $[Y_{\pi}^{\bullet}GGG]^+$ (Figure 1d) and $[W_{\pi}^{\bullet}GG]^+$ systems (Figure S5b).

Experimental and theoretical investigations of the structures of the $[c_1 - 17]^+$ and $[b_2 - H - 17]^{\bullet+}$ ions

Labeling experiments. In order to investigate the structures and details of the mechanisms by which the $[c_1 - 17]^+$ and $[b_2 - H - 17]^{\bullet+}$ ions are formed, isotopic-labeling experiments were carried out. The $[c_1 - 17]^+$ ion derived from $[Y_{\pi}^{\bullet}GG]^+$, molecular formula $C_9NO_2H_8^+$, contains only one nitrogen and this could originate either at the N-terminus or the first amide bond. The spectrum in Figure 3a establishes that it is the nitrogen of the amide bond that is retained and

also provides support for the premise that the $[c_1 - 17]^+$ ion is formed via the $[z_3 - H]^{\bullet+}$ ion. The ^{15}N is also retained in the $[b_2 - H - 17]^{\bullet+}$ ion and the CID spectrum of the labeled $[z_3 - H]^{\bullet+}$ ion, shown in Figure 3b, has only the $[c_1 - 17]^+$ and $[b_2 - H - 17]^{\bullet+}$ ions as abundant product ions.

Fragmentation of *d4*-$[Y_\pi^\bullet GG]^+$ (Figure 3c), where the four aromatic hydrogens atoms of the phenol ring have been replaced by deuterium atoms, resulted in a spectrum where all the product ions have mass-to-charge values higher by 4 relative to the unlabeled peptide, with one notable exception: the $[b_2 - H - 17]^{\bullet+}$ ion observed at *m/z* 203 in the spectrum of $[Y_\pi^\bullet GG]^+$ is shifted to *m/z* 206 in the spectrum of *d4*-$[Y_\pi^\bullet GG]^+$ showing that one of the aromatic deuteriums was lost in the formation of this ion. Confirmation of the involvement of the aromatic ring is further indicated by the spectrum of the $[c_1 - 17]^+$ ion of *d4*-$[Y_\pi^\bullet GG]^+$ (Figure 3g), where the loss of water is HDO and not H_2O. In order to further probe the exact bonding site in the aromatic ring, the CID spectra of *d2*-$[Y_\pi^\bullet GG]^+$, where the aromatic hydrogens at the 3- and 5-positions have been replaced by deuteriums, and its fragment ion $[z_3 - H]^{\bullet+}$ were examined (Figures 3e and 3f). *All* the fragment ions were found to have mass-to-charge ratios higher by 2, indicating that the deuteriums from positions 3 and 5 were not lost in the formation of either the $[b_2 - H - 17]^{\bullet+}$ or $[c_1 - 17]^+$ ion. Fragmentation of the $[c_1 - 17]^+$ ion derived from *d2*-$[Y_\pi^\bullet GG]^+$ resulted in the loss of H_2O (18 Da), (Figure 3h) demonstrating that any interaction between the backbone and the aromatic ring had not involved the two deuterium atoms on the ε-carbons of the ring.

Theoretical investigations. We used the prototypical radical cationic tyrosylglycylglycine to examine the potential energy surface for isomers of the $[c_1 - 17]^+$ and $[b_2 - H - 17]^{\bullet+}$ ion. Nine structures were optimized for the $[c_1 - 17]^+$ and the two in which a heteroatom from the backbone is covalently bound to the aromatic ring were found to have much lower energies than all the other isomers (Figure S6).

Two pathways involving nucleophilic attack on the aromatic ring of the $[z_3 - H]^{\bullet+}$ ion by either the amide oxygen (O-attacking) or the amide nitrogen (N-attacking) have been examined in detail for the $[Y_\pi^\bullet GG]^+$ system. The key steps are summarized in Scheme 1 (a more detailed version showing step-by-step details is provided in Scheme S1). All energies discussed are

enthalpies in kcal mol^{-1}at 0 K. Free energies at 298 K are also provided in the schemes in parentheses. All energies are relative to the lowest-energy canonical structure for $[Y_{\pi}^{\bullet}GG]^{+}$ in which both the radical and charge are located in the π-system of the tyrosine residue. The upper numbers, given in bold type, are from M06-2X/6-31++G(d,p) calculations and the lower numbers are from B3LYP calculations with the same basis set. Both sets of calculations show the formation of the $[z_3 - H]^{\bullet+}$ ion (structure **1a**, Scheme 1) to be endothermic but there are significant differences in the calculated energies.

Nucleophilic attack by either a nitrogen or a carbonyl oxygen on the aromatic ring of the $[z_3 - H]^{\bullet+}$ ion of $[Y_{\pi}^{\bullet}GG]^{+}$ requires that the structure adopting the higher energy *cis* conformation about the $C_{\alpha}=C_{\beta}$ bond of the tyrosine residue (structure **1b**). In our initial calculations using the B3LYP functional, we found that the nucleophilic attack by the carbonyl oxygen (giving structure 7) has a low energy barrier (8.9 kcal mol^{-1} relative to **1b**), and considerably lower than that for the attack by the amide nitrogen (giving structure **2**, with a barrier of 21.9 kcal mol^{-1}). However, subsequent rearrangement of **7** involving proton transfers have higher barriers than those for the formation and rearrangements of **2**, strongly suggesting that dissociation via **2** is the more probable pathway.

Rearrangement of ion **2** into **3** via a series of proton shifts has an overall barrier of only 7.6 kcal mol^{-1} as determined by B3LYP level and subsequent cleavage of the $N–C_{\alpha}$ bond of the central residue to give the $[c_1 - 17]^{+}$ ion (structure **5a**) and the N-acetyl-glycine radical has a barrier that is 10.1 kcal mol^{-1} lower than that for conversion of **2** into **3**. In this mechanism, the aromatic hydrogen that was displaced by the initial nucleophilic attack is relocated to the nitrogen of the product, protonated 2,7-dihydroxyquinoline.

The $[b_2 - H - 17]^{\bullet+}$ ion (structure **6a**) may also be formed from structure **2** by 1,4 proton migration of the aromatic hydrogen to the amide nitrogen followed by loss of glycine. This mechanism accounts for the formation of $[b_2 - D - 17]^{\bullet+}$ ion, but the barrier to this dissociation is 23.9 kcal mol^{-1} and, on the overall profile is 9.3 kcal mol^{-1} higher than the barrier for conversion of **1b** into **2**. By contrast, on the pathway to the formation of the $[c_1 - 17]^{+}$ ion conversion of **1b**

into **2** has the highest barrier. Consequently, the B3LYP calculations lead to the conclusion that at low collision energies the $[c_1 - 17]^+$ ion should be the dominant product. This is not consistent with the experimental observation that *both* $[c_1 - 17]^+$ and $[b_2 - H - 17]^{\bullet+}$ ions are always in high abundance.

All the structures in Scheme 1 were re-optimized using the M06-2X functional and the picture is somewhat modified. The barrier to conversion of the *trans* isomer **1a** into the *cis* isomer **1b** is almost unchanged (22.0 kcal mol^{-1} compared with 22.8 kcal mol^{-1} from the B3LYP calculation) but the transition state for this step was *higher* in energy than all the subsequent barriers leading to both $[c_1 - 17]^+$ and $[b_2 - H - 17]^{\bullet+}$ ions via the mechanism involving nucleophilic attack by the amide nitrogen on the aromatic ring. Consequently, when sufficient energy is provided to form **1b**, in the absence of any collisional stabilization, both product ions should be observed. Ring closure by using the carbonyl oxygen as the nucleophile is again disfavored as the barriers to the proton transfer steps after the initial formation of **7** are higher than that for conversion of **1a** into **1b**.

The structure proposed for the $[c_1 - 17]^+$ ion (**5a**) is protonated 2,7-dihydroxyquinoline. Recalling the CID experiment on the $[c_1 - 17]^+$ ion showed it to lose a water molecule (**Figure 1c**); support for the proposed structure was provided by the fact that an authentic sample of protonated 2,7-dihydroxyquinoline similarly lost water (Figure S7).

Applications in long peptide sequence with different radical sites

In addition to studying tripeptide radical cations possessing an aromatic amino acid residue at the N-terminus, we extended the investigation to systematically elucidate the structural features influencing the rearrangement process. Formation of residue-specific fragment ions $[c_1 - 17]^+$ at *m/z* 162, 185 and $[b_2 - H - 17]^{\bullet+}$ at *m/z* 203, 226 is evidently prevalent from many tyrosine- and tryptophan-containing peptide radical cations (Figure S8 and S9). In addition to ions with the charge and spin delocalized over a π-system, the specific fragment ions $[c_1 - 17]^+$ and $[b_2 - H - 17]^{\bullet+}$ are also be observed in the CID of $[YGG_\alpha^\bullet]^+$, $[YG_\alpha^\bullet G]^+$ and $[Y_\varepsilon^\bullet GG]^+$ ions where the radical

is located at different positions.[62]

We also investigated a variety of peptide cationic analogues from tripeptides to larger oligopeptides containing a tyrosine or a tryptophan residue at different positions along the peptide backbone of ions $[G_mXG_n]^{\bullet+}$ (m=0-3, n=2−5, X=Y or W). Table 1 displays the relative abundances of $[z_n - H]^{\bullet+}$, $[c_1 - 17]^+$ and $[b_2 - H - 17]^{\bullet+}$ ions observed in the fragmentations of peptide radical cations containing one tyrosine or one tryptophan residue (denoted $M^{\bullet+}$). All the tyrosine- and tryptophan-containing peptide radical cations produced fragment ions $[z_n - H]^{\bullet+}$, most of which are in relatively high abundance. The product $[z_n - H]^{\bullet+}$ ions were isolated and the last two columns in Table 1 give the relative abundances of $[c_1 - 17]^+$ and $[b_2 - H - 17]^{\bullet+}$ ions produced in the fragmentations of these ions. Clearly the $[c_1 - 17]^+$ and $[b_2 - H - 17]^{\bullet+}$ ions are dominant products in the dissociations of the $[z_n - H]^{\bullet+}$ ions. Additionally, we varied the middle residue of $[Y_\pi^{\bullet}XG]^+$ to include several aliphatic amino acid residues (i.e., X = A, V, L, P) to examine the effect of the residue adjacent to the aromatic residue. The CID spectra of YAG, YVG, YLG and YPG all showed abundant $[z_3 - H]^{\bullet+}$ ions and the MS/MS on these $[z_3 - H]^{\bullet+}$ ions produced abundant $[b_2 - H - 17]^{\bullet+}$ ions and some $[c_1 - 17]^+$ ions (Figure S9). In general, the observation of a $[z_n - H]^{\bullet+}$ ion indicates the presence and the position of an aromatic residue in a peptide chain, and the residue-specific product ion $[c_1 - 17]^+$ identifies the aromatic residue. The $[b_2 - H - 17]^{\bullet+}$ ions provide information on what residue is adjacent to the aromatic residue.

Conclusions

Novel residue-specific fragment ions $[c_1 - 17]^+$ at *m/z* 162 and 185, and $[b_2 - H - 17]^{\bullet+}$ at *m/z* 203, and 226 are present in the low-energy CID of a series of tyrosine- and tryptophan-containing peptide radical cations, respectively. Using $[Y_\pi^{\bullet}GG]^+$ as a model system, the mechanisms for the formations of these ions has been investigated by isotopic labeling experiments and DFT calculations. The results reveal an unprecedented rearrangement involving nucleophilic attack by a backbone amide nitrogen atom on the δ-carbon of the tyrosine residue; it is followed by several proton transfer steps culminating in the cleavage of either the N–C_α or the

second amide bond to produce the $[c_1 - 17]^+$ and $[b_2 - H - 17]^{\bullet+}$ ions respectively. Elimination of either an ammonia molecule or an amide from the N-terminus to produce $[z_n - H]^{\bullet+}$ ions is an essential step that precedes formation of these residue-specific ions. This study provides a fundamental understanding of a novel cyclization reaction between peptide backbone nitrogen and aromatic side chains. The observation of $[c_1 - 17]^+$ and $[b_2 - H - 17]^{\bullet+}$ ions along with the *m/z* value of the $[z_n - H]^{\bullet+}$ ion can provide peptide sequencing information by identification of an aromatic residue and establishing what amino acid is attached to C-terminal side of the aromatic residue.

Acknowledgments

This study was supported by the Hong Kong Research Grants Council (HKU17306015 and HKU701613) and Natural Sciences and Engineering Research Council (NSERC) of Canada and is made possible by the facilities of the Shared Hierarchical Academic Research Computing Network (http://www.sharcnet.ca).

References

1. R. Aebersold and M. Mann, *Nature*, 2003, **422**, 198-207.
2. J. T. Stults and D. Arnott, in *Methods Enzymol.*, ed. A. L. Burlingame, Academic Press, 2005, vol. 402, pp. 245-289.
3. N. L. Kelleher, *Anal. Chem.*, 2004, **76**, 196 A-203 A.
4. V. H. Wysocki, G. Cheng, Q. Zhang, K. A. Herrmann, R. L. Beardsley and A. E. Hilderbrand, in *Principles of Mass Spectrometry Applied to Biomolecules*, eds. J. Laskin and C. Lifshitz, Wiley Interscience, New York, 2006, ch. 8, pp. 279-300.
5. V. H. Wysocki, G. Tsaprailis, L. L. Smith and L. A. Breci, *J. Mass Spectrom.*, 2000, **35**, 1399-1406.
6. B. Paizs and S. Suhai, *Mass Spectrom. Rev.*, 2005, **24**, 508-548.
7. G. Tsaprailis, H. Nair, Á. Somogyi, V. H. Wysocki, W. Zhong, J. H. Futrell, S. G. Summerfield and S. J. Gaskell, *J. Am. Chem. Soc.*, 1999, **121**, 5142-5154.
8. O. Burlet, R. S. Orkiszewski, K. D. Ballard, S. J. Gaskell and M. Bertrand, *Rapid Commun. Mass Spectrom.*, 1992, **6**, 658-662.
9. J. L. Jones, A. R. Dongré, Á. Somogyi and V. H. Wysocki, *J. Am. Chem. Soc.*, 1994, **116**, 8368-8369.
10. A. R. Dongré, J. L. Jones, Á. Somogyi and V. H. Wysocki, *J. Am. Chem. Soc.*, 1996, **118**, 8365-8374.
11. R. A. Zubarev, *Mass Spectrom. Rev.*, 2003, **22**, 57-77.
12. R. A. Zubarev, *Curr. Opin. Biotechnol.*, 2004, **15**, 12-16.
13. F. Tureček, *Mass Spectrom. Rev.*, 2007, **26**, 563-582.
14. A. C. Hopkinson, *Mass Spectrom. Rev.*, 2009, **28**, 655-671.
15. K. O. Zhurov, L. Fornelli, M. D. Wodrich, Ü. A. Laskay and Y. O. Tsybin, *Chem. Soc. Rev.*, 2013, **42**, 5014-5030.
16. F. Tureček and R. R. Julian, *Chem. Rev.*, 2013, **113**, 6691-6733.
17. I. K. Chu and J. Laskin, *Eur. J. Mass Spectrom.*, 2011, **17**, 543-556.
18. I. K. Chu, C. F. Rodriquez, T. C. Lau, A. C. Hopkinson and K. W. M. Siu, *J. Phys. Chem. B*, 2000, **104**, 3393-3397.
19. A. C. Hopkinson and K. W. M. Siu, in *Principles of Mass Spectrometry Applied to Biomolecules*, eds. J. Laskin and C. Lifshitz, Wiley Interscience, New York, 2006, ch. 9, pp. 301-335.
20. T. Ly and R. R. Julian, *J. Am. Chem. Soc.*, 2008, **130**, 351-358.
21. J. Laskin, Z. B. Yang, C. Lam and I. K. Chu, *Anal. Chem.*, 2007, **79**, 6607-6614.
22. F. McLafferty, D. Horn, K. Breuker, Y. Ge, M. Lewis, B. Cerda, R. Zubarev and B. Carpenter, *J. Am. Soc. Mass Spectrom.*, 2001, **12**, 245-249.
23. J. E. P. Syka, J. J. Coon, M. J. Schroeder, J. Shabanowitz and D. F. Hunt, *Proc. Natl. Acad. Sci. U. S. A.*, 2004, **101**, 9528-9533.
24. Y. Ke, U. H. Verkerk, P. Y. I. Shek, A. C. Hopkinson and K. W. M. Siu, *J. Phys. Chem. B*, 2006, **110**, 8517-8523.
25. S. Wee, R. A. J. O'Hair and W. D. McFadyen, *Int. J. Mass Spectrom.*, 2006, **249**, 171-183.
26. E. Bagheri-Majdi, Y. Y. Ke, G. Orlova, I. K. Chu, A. C. Hopkinson and K. W. M. Siu, *J. Phys. Chem. B*, 2004, **108**, 11170-11181.
27. C. K. Siu, Y. Ke, G. Orlova, A. C. Hopkinson and K. W. M. Siu, *J. Am. Soc. Mass Spectrom.*, 2008, **19**,

1799-1807.
28. D. C. M. Ng, T. Song, S. O. Siu, C. K. Siu, J. Laskin and I. K. Chu, *J. Phys. Chem. B*, 2010, **114**, 2270-2280.
29. T. Song, D. C. M. Ng, Q. Quan, C.-K. Siu and I. K. Chu, *Chem.-Asian J.*, 2011, **6**, 888-898.
30. J. Laskin, Z. Yang, C. M. D. Ng and I. K. Chu, *J. Am. Soc. Mass Spectrom.*, 2010, **21**, 511-521.
31. J. Zhao, T. Song, M. Xu, Q. Quan, K. W. M. Siu, A. C. Hopkinson and I. K. Chu, *Phys. Chem. Chem. Phys.*, 2012, **14**, 8723-8731.
32. S. Wee, R. A. J. O'Hair and W. D. McFadyen, *Int. J. Mass Spectrom.*, 2004, **234**, 101-122.
33. M. Xu, T. Song, Q. Quan, Q. Hao, D. C. Fang, C. K. Siu and I. K. Chu, *Phys. Chem. Chem. Phys.*, 2011, **13**, 5888-5896.
34. T. Ly and R. R. Julian, *J. Am. Soc. Mass Spectrom.*, 2009, **20**, 1148-1158.
35. Y. Z. Ouyang, Y. Z. Liang, S. H. Li, X. Luo, L. X. Zhang, Z. H. Tang and X. N. Xu, *Int. J. Mass Spectrom.*, 2009, **286**, 112-121.
36. T. Song, Q. Hao, C.-H. Law, C.-K. Siu and I. Chu, *J. Am. Soc. Mass Spectrom.*, 2012, **23**, 264-273.
37. T. Song, C.-Y. Ma, I. K. Chu, C.-K. Siu and J. Laskin, *J. Phys. Chem. A*, 2013, **117**, 1059.
38. Q. Hao, T. Song, D. C. M. Ng, Q. Quan, C.-K. Siu and I. K. Chu, *J. Phys. Chem. B*, 2012, **116**, 7627-7634.
39. I. K. Chu, C.-K. Siu, J. K.-C. Lau, W. K. Tang, X. Mu, C. K. Lai, X. Guo, X. Wang, N. Li and Y. Xia, *Int. J. Mass Spectrom.*, 2015, **390**, 24-27.
40. M. Valko, D. Leibfritz, J. Moncol, M. T. Cronin, M. Mazur and J. Telser, *Int J Biochem Cell Biol*, 2007, **39**, 44-84.
41. W. Droge, *Physiol. Rev.*, 2002, **82**, 47-95.
42. V. J. Thannickal and B. L. Fanburg, *Am. J. Physiol.-Lung Cell. Mol. Physiol.*, 2000, **279**, L1005-L1028.
43. M. J. Davies and R. T. Dean, *Radical-mediated protein oxidation: from chemistry to medicine*, Oxford University Press, 1997.
44. R. T. Dean, S. L. Fu, R. Stocker and M. J. Davies, *Biochem. J.*, 1997, **324**, 1-18.
45. C. L. Hawkins and M. J. Davies, *Biochimica et Biophysica Acta, Bioenergetics*, 2001, **1504**, 196-219.
46. R. T. Dean, J. V. Hunt, A. J. Grant, Y. Yamamoto and E. Niki, *Free Radical Biol. Med.*, 1991, **11**, 161-168.
47. S. P. Wolff, A. Garner and R. T. Dean, *Trends Biochem. Sci.*, 1986, **11**, 27-31.
48. K. K. Griendling, D. Sorescu, B. Lassegue and M. Ushio-Fukai, *Arterioscler. Thromb. Vasc. Biol.*, 2000, **20**, 2175-2183.
49. B. Giese, M. Napp, O. Jacques, H. Boudebous, A. M. Taylor and J. Wirz, *Angew. Chem.*, 2005, **117**, 4141-4143.
50. M. Faraggi, M. R. DeFelippis and M. H. Klapper, *J. Am. Chem. Soc.*, 1989, **111**, 5141-5145.
51. C. Aubert, M.H. Vos, P. Mathis, A.P. Eker and K. Bretel, *Nature*, 2000, **405**, 586-590.
52. W. C. Chan and P. D. White, *Fmoc Solid Phase Peptide Synthesis: A Practical Approach*, Oxford University Press, New York, 2000.
53. SPARTAN, '04 Essential V2.0.0; Wavefunction, Inc.: Irvine, CA,2004.
54. A. D. Becke, *J. Chem. Phys.*, 1993, **98**, 5648-5652.
55. C. Lee, W. Yang and R. G. Parr, *Phys. Rev. B*, 1988, **37**, 785.
56. W. J. Hehre, R. Ditchfield and J. A. Pople, *J. Chem. Phys.*, 1972, **56**, 2257-2261.
57. T. Clark, J. Chandrasekhar, G. W. Spitznagel and P. v. R. Schleyer, *J. Comput. Chem.*, 1983, **4**, 294-301.
58. C. Gonzalez and H. B. Schlegel, *J. Chem. Phys.* 1989, **90**, 2154-2161.

59. Y. Zhao, N. E. Schultz and D. Truhlar, *J. Chem. Phys.*, 2005, **123**, 161103.
60. Y. Zhao and D. G. Truhlar, *Theor. Chem. Acc.*, 2008, **120**, 215-241.
61. M. J. Frisch, G. W. Trucks, H. B. Schlegel, G. E. Scuseria, M. A. Robb, J. R. Cheeseman, G. Scalmani, V. Barone, B. Mennucci, G. A. Petersson, H. Nakatsuji, M. Caricato, X. Li, H. P. Hratchian, A. F. Izmaylov, J. Bloino, G. Zheng, J. L. Sonnenberg, M. Hada, M. Ehara, K. Toyota, R. Fukuda, J. Hasegawa, M. Ishida, T. Nakajima, Y. Honda, O. Kitao, H. Nakai, T. Vreven, J. A. Montgomery, Jr., J. E. Peralta, F. Ogliaro, M. Bearpark, J. J. Heyd, E. Brothers, K. N. Kudin, V. N.Staroverov, R. Kobayashi, J. Normand, K. Raghavachari, A. Rendell, J. C.Burant, S. S. Iyengar, J. Tomasi, M. Cossi, N. Rega, N. J. Millam, M. Klene, J. E. Knox, J. B. Cross, V. Bakken, C. Adamo, J. Jaramillo, R. Gomperts, R. E. Stratmann, O. Yazyev, A. J. Austin, R. Cammi, C. Pomelli, J. W. Ochterski, R. L. Martin, K. Morokuma, V. G. Zakrzewski, G. A. Voth, P. Salvador, J. J. Dannenberg, S. Dapprich, A. D. Daniels, Ö. Farkas, J. B. Foresman, J. V. Ortiz, J. Cioslowski, D. J. Fox, , *Gaussian 09, Revision D.01*, Gaussian, Inc., Wallingford CT, 2009.
62. C.-K. Lai, X. Mu, Q. Hao, A. C. Hopkinson and I. K. Chu, *Phys. Chem. Chem. Phys.*, 2014, **16**, 24235-24243.

Caption for scheme:

Scheme 1: Schematic diagram showing the formations of $[c_1 - 17]^+$ and $[b_2 - H - 17]^{\bullet+}$ ions from $[YGG]^{\bullet+}$ via nucleophilic attack by backbone nitrogen or oxygen. Upper numbers are the relative enthalpies (ΔH^o_0) and free energies (ΔG^o_{298}, in parenthesis) calculated at M06-2X/6-31++G(d,p) level while the lower numbers are those calculated at the B3LYP/6-31++G(d,p) level. All energies are in kcal mol^{-1}.

Captions for figures:

Figure 1. CID spectra of (a) $[Y_\pi^\bullet GGG]^+$; and the MS/MS spectra of the product ions at (b) *m/z* 335 corresponding to $[z_4 - H]^{\bullet+}$, (c) *m/z* 162 corresponding to $[c_1 - 17]^+$, and (d) *m/z* 203 corresponding to $[b_2 - H - 17]^{\bullet+}$ ions.

Figure 2. CID spectra of (a) $[W_\pi^\bullet GG]^+$ and (b) $[z_3 - H]^{\bullet+}$ ions derived from $[W_\pi^\bullet GG]^+$; and CID spectra of (c) $[FGG_\alpha^\bullet]^+$ and (d) $[z_3 - H]^{\bullet+}$ ions derived from $[FGG_\alpha^\bullet]^+$.

Figure 3. CID spectra of labeled $[Y_\pi^\bullet GG]^+$ and $[z_3 - H]^{\bullet+}$ radical cations: (a) and (b) the first amide nitrogen is labeled by ^{15}N isotope, (c) and (d) the aromatic hydrogens in tyrosine are replaced by deuteriums, and (e) and (f) the aromatic hydrogens at 3- and 5-positions of tyrosine are replaced by deuteriums; and CID spectra of $[c_1 - 17]^+$ ion from (g) *d4*-$[Y_\pi^\bullet GG]^+$ and (h) *d2*-$[Y_\pi^\bullet GG]^+$.

Table 1. Relative abundances (%) of $[c_1 - 17]^+$, $[b_2 - H - 17]^{\bullet+}$ and $[z_n - H]^{\bullet+}$ ions generated from tyrosine- and tryptophan-containing peptide radical cations, $M^{\bullet+}$; $[c_1 - 17]^+$ and $[b_2 - H - 17]^{\bullet+}$ ions derived from $[z_n - H]^{\bullet+}$ ions.

	From $M^{\bullet+}$			From $[z_n - H]^{\bullet+}$	
Peptide	$[c_1 - 17]^+$	$[b_2 - H - 17]^{\bullet+}$	$[z_n - H]^{\bullet+}$	$[c_1 - 17]^+$	$[b_2 - H - 17]^{\bullet+}$
YGG	10	38	30	90	100
YGGG	18	9	50	100	98
YGGGG	8	8	38	65	68
YGGGGG	8	3	14	42	12
GYGG	18	18	100	100	100
GYGGG	90	100	60	75	100
GYGGGG	58	60	100	70	50
GGYGG	8	12	18	100	80
GGYGGG	75	70	20	23	30
GGGYGG	2	2	5	40	50
WGG	5	10	100	30	100
WGGG	30	82	100	30	100
WGGGG	5	6	100	60	100
WGGGGG	4	3	100	45	55
GWGG	7	48	100	40	100
GWGGG	23	100	15	20	100
GWGGGG	30	40	90	70	80
GGWGG	30	100	100	40	100
GGWGGG	25	100	65	30	100
GGGWGG	4	3	60	30	75

Scheme 1.

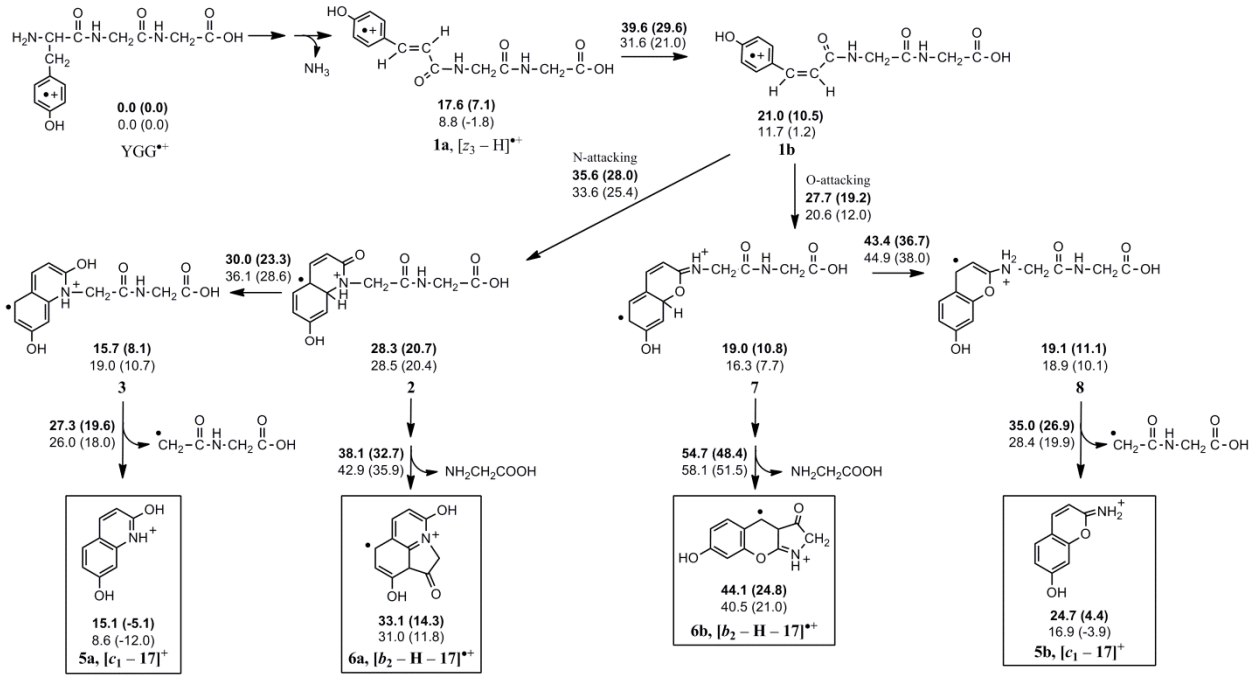
0.0 (0.0)
0.0 (0.0)
YGG•+
NH3
17.6 (7.1)
8.8 (-1.8)
1a, [z3 – H]•+
39.6 (29.6)
31.6 (21.0)
21.0 (10.5)
11.7 (1.2)
1b
N-attacking
35.6 (28.0)
33.6 (25.4)
O-attacking
27.7 (19.2)
20.6 (12.0)
30.0 (23.3)
36.1 (28.6)
43.4 (36.7)
44.9 (38.0)
15.7 (8.1)
19.0 (10.7)
3
28.3 (20.7)
28.5 (20.4)
2
19.0 (10.8)
16.3 (7.7)
7
19.1 (11.1)
18.9 (10.1)
8
27.3 (19.6)
26.0 (18.0)
38.1 (32.7)
42.9 (35.9)
NH2CH2COOH
54.7 (48.4)
58.1 (51.5)
NH2CH2COOH
35.0 (26.9)
28.4 (19.9)
15.1 (-5.1)
8.6 (-12.0)
5a, |c1 – 17|+
33.1 (14.3)
31.0 (11.8)
6a, |b2 – H – 17|•+
44.1 (24.8)
40.5 (21.0)
6b, |b2 – H – 17|•+
24.7 (4.4)
16.9 (-3.9)
5b, |c1 – 17|+

Figure 1

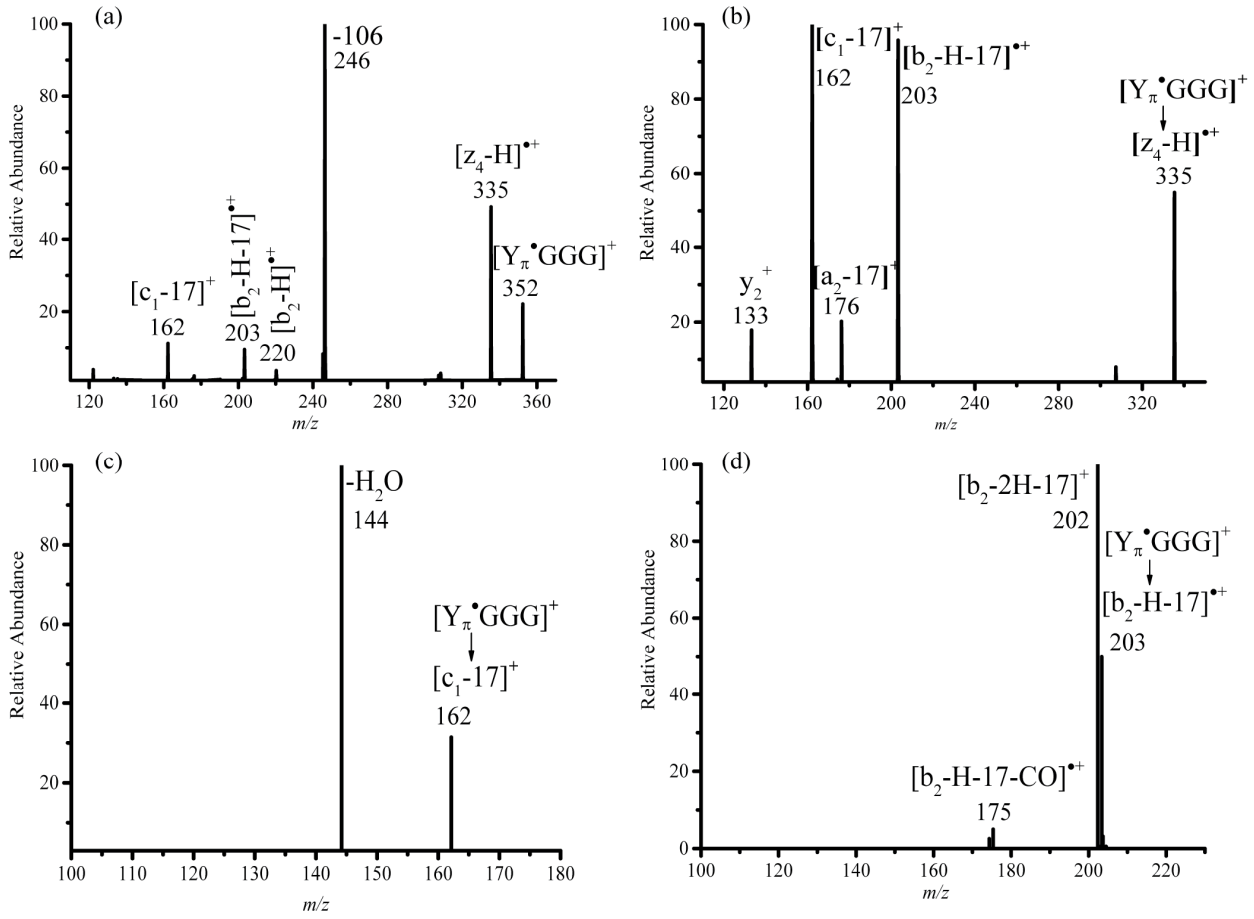
(a)
-106
246
[z4-H]•+
335
[Yπ•GGG]+
352
[b2-H-17]•+
203
[b2-H]•+
220
[c1-17]+
162
Relative Abundance
m/z
(b)
[c1-17]+
162
[b2-H-17]•+
203
[Yπ•GGG]+
[z4-H]•+
335
y2+
133
[a2-17]+
176
Relative Abundance
m/z
(c)
-H2O
144
[Yπ•GGG]+
[c1-17]+
162
Relative Abundance
m/z
(d)
[b2-2H-17]+
202
[Yπ•GGG]+
[b2-H-17]•+
203
[b2-H-17-CO]•+
175
Relative Abundance
m/z

Figure 2.

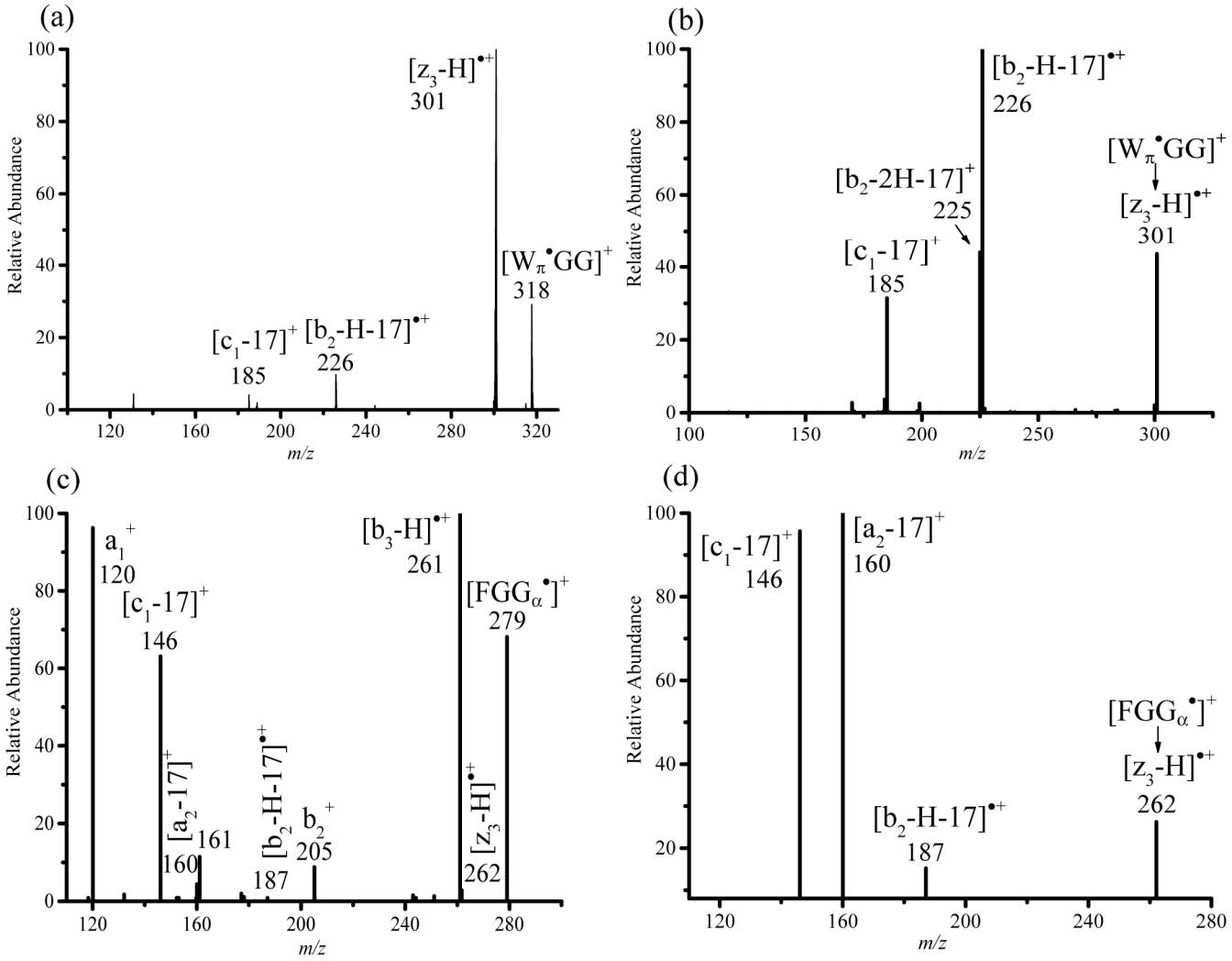
(a)
[z3-H]•+
301
[Wπ•GG]+
318
[c1-17]+
185
[b2-H-17]•+
226
Relative Abundance
m/z
(b)
[b2-H-17]•+
226
[Wπ•GG]+
[z3-H]•+
301
[b2-2H-17]+
225
[c1-17]+
185
Relative Abundance
m/z
(c)
a1+
120
[c1-17]+
146
[a2-17]+
160
161
[b2-H-17]•+
187
b2+
205
[b3-H]•+
261
[FGGα•]+
279
[z3-H]•+
262
Relative Abundance
m/z
(d)
[c1-17]+
146
[a2-17]+
160
[FGGα•]+
[z3-H]•+
262
[b2-H-17]•+
187
Relative Abundance
m/z

Figure 3.

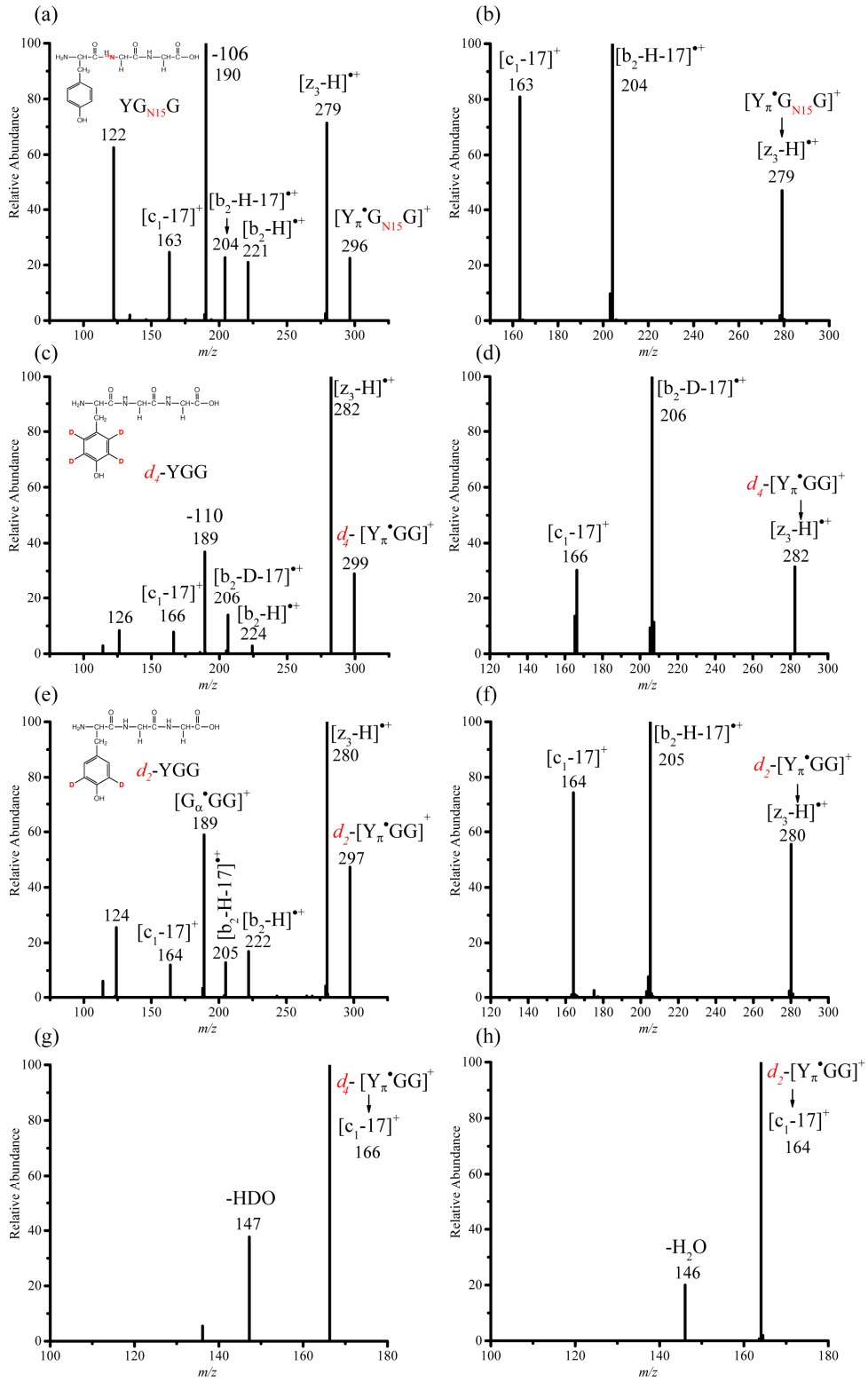
(a)
YG$_{N15}$G
122
-106
190
[z$_3$-H]$^{\bullet+}$
279
[c$_1$-17]$^+$
163
[b$_2$-H-17]$^{\bullet+}$
204
[b$_2$-H]$^{\bullet+}$
221
[Y$_\pi^\bullet$G$_{N15}$G]$^+$
296
(b)
[c$_1$-17]$^+$
163
[b$_2$-H-17]$^{\bullet+}$
204
[Y$_\pi^\bullet$G$_{N15}$G]$^+$
[z$_3$-H]$^{\bullet+}$
279
(c)
d_4-YGG
[z$_3$-H]$^{\bullet+}$
282
-110
189
d_4- [Y$_\pi^\bullet$GG]$^+$
299
[c$_1$-17]$^+$
166
[b$_2$-D-17]$^{\bullet+}$
206
126
[b$_2$-H]$^{\bullet+}$
224
(d)
[b$_2$-D-17]$^{\bullet+}$
206
d_4-[Y$_\pi^\bullet$GG]$^+$
[z$_3$-H]$^{\bullet+}$
282
[c$_1$-17]$^+$
166
(e)
d_2-YGG
[G$_\alpha^\bullet$GG]$^+$
189
[z$_3$-H]$^{\bullet+}$
280
d_2-[Y$_\pi^\bullet$GG]$^+$
297
124
[c$_1$-17]$^+$
164
[b$_2$-H-17]$^{\bullet+}$
205
[b$_2$-H]$^{\bullet+}$
222
(f)
[c$_1$-17]$^+$
164
[b$_2$-H-17]$^{\bullet+}$
205
d_2-[Y$_\pi^\bullet$GG]$^+$
[z$_3$-H]$^{\bullet+}$
280
(g)
d_4- [Y$_\pi^\bullet$GG]$^+$
[c$_1$-17]$^+$
166
-HDO
147
(h)
d_2-[Y$_\pi^\bullet$GG]$^+$
[c$_1$-17]$^+$
164
-H$_2$O
146
Relative Abundance
m/z

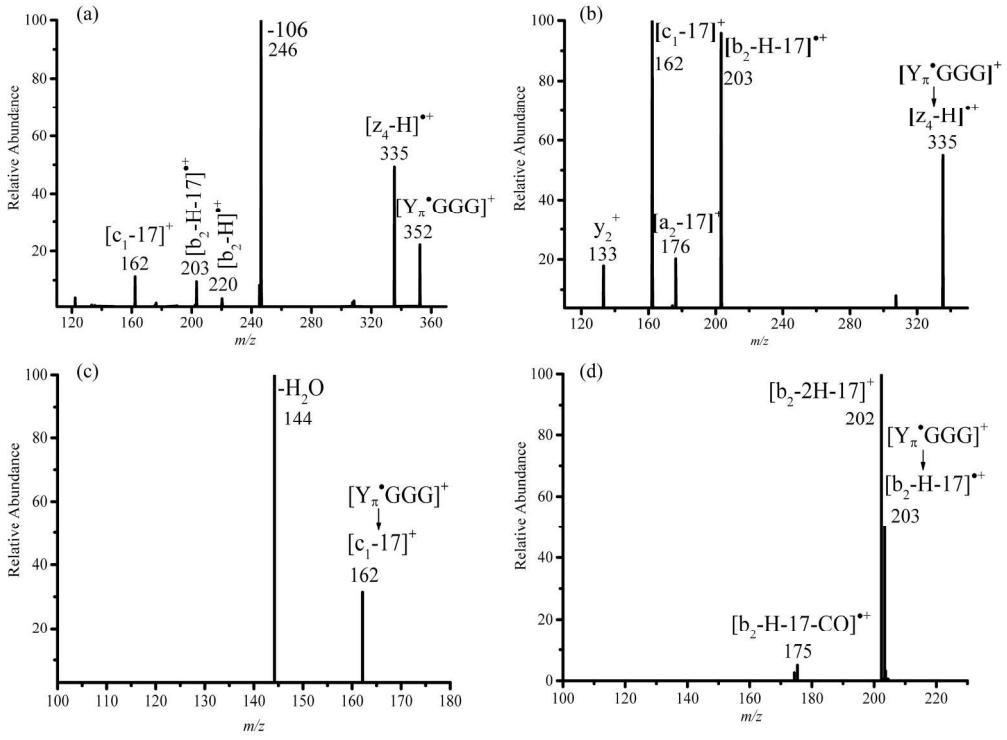

CID spectra of (a) $[Y_n^{\bullet}GGG]^+$; and the MS/MS spectra of the product ions at (b) *m/z* 335 corresponding to $[z_4 - H]^{\bullet+}$, (c) *m/z* 162 corresponding to $[c_1 - 17]^+$, and (d) *m/z* 203 corresponding to $[b_2 - H - 17]^{\bullet+}$ ions.
177x130mm (300 x 300 DPI)

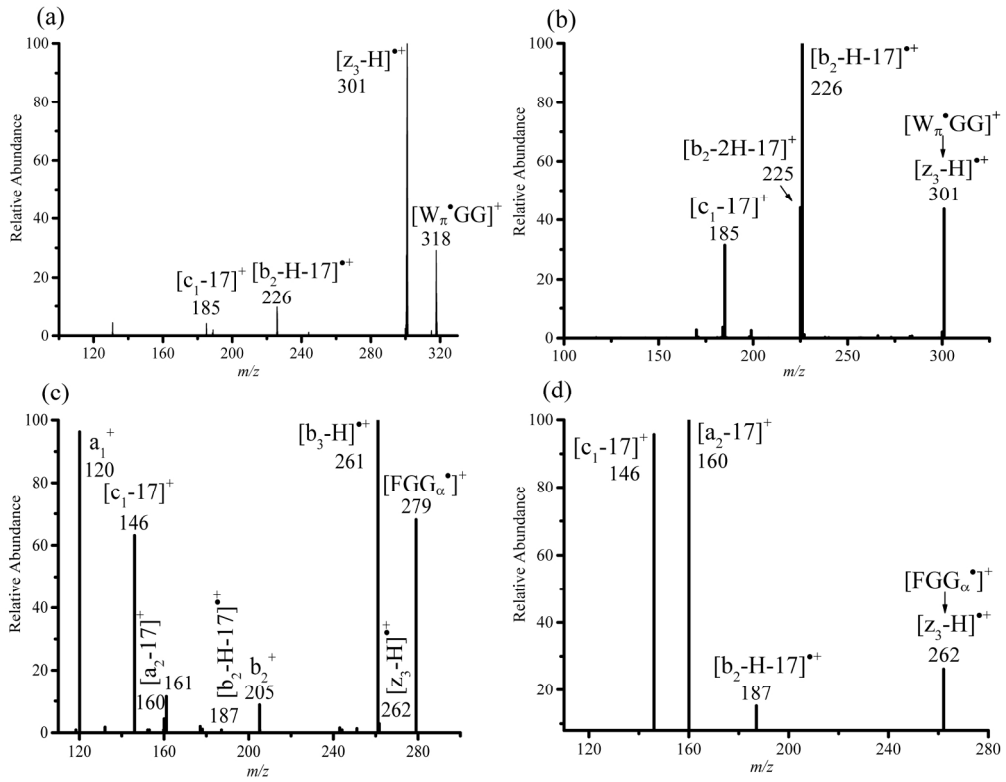

CID spectra of (a) $[W_{\pi}^{\bullet}GG]^{+}$ and (b) $[z_3 - H]^{\bullet+}$ ions derived from $[W_{\pi}^{\bullet}GG]^{+}$; and CID spectra of (c) $[FGG_{\alpha}^{\bullet}]^{+}$ and (d) $[z_3 - H]^{\bullet+}$ ions derived from $[FGG_{\alpha}^{\bullet}]^{+}$.
177x138mm (300 x 300 DPI)

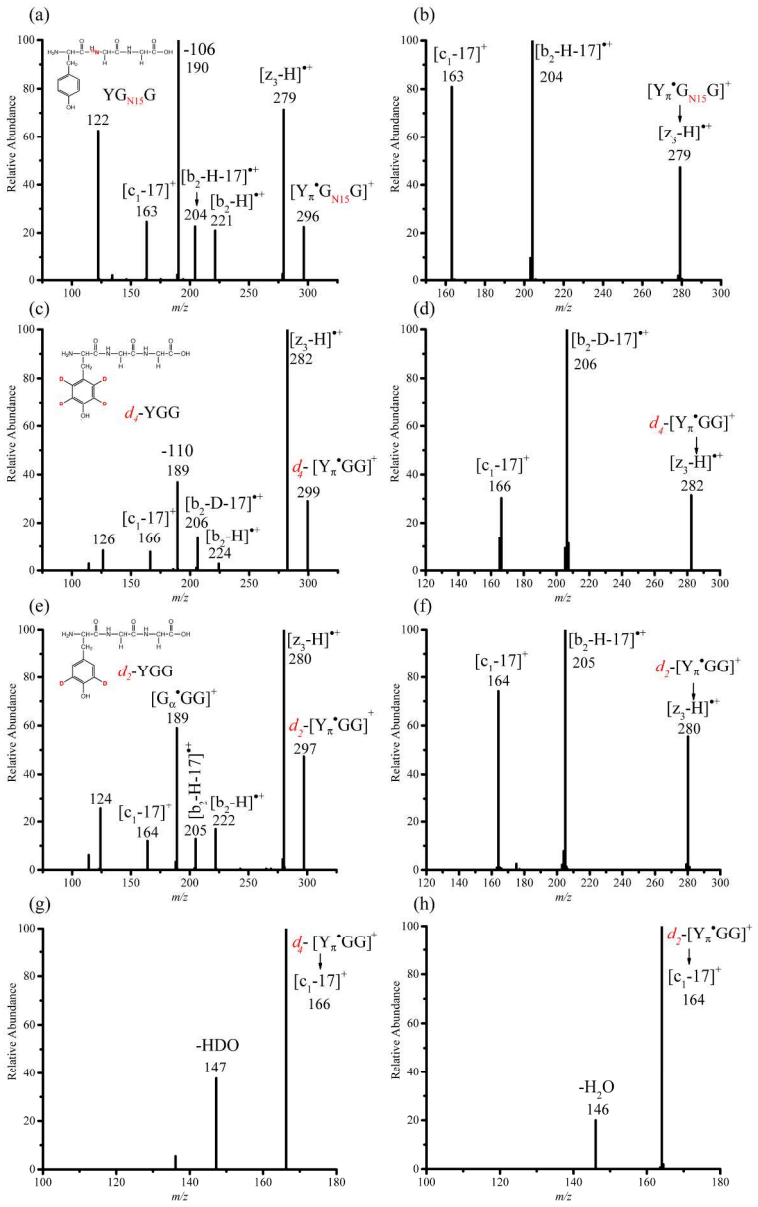

CID spectra of labeled $[Y_n^{\bullet}GG]^+$ and $[z_3 - H]^{\bullet+}$ radical cations: (a) and (b) the first amide nitrogen is labeled by ^{15}N isotope, (c) and (d) the aromatic hydrogens in tyrosine are replaced by deuteriums, and (e) and (f) the aromatic hydrogens at 3- and 5-positions of tyrosine are replaced by deuteriums; and CID spectra of $[c_1 - 17]^+$ ion from (g) *d4*-$[Y_n^{\bullet}GG]^+$ and (h) *d2*-$[Y_n^{\bullet}GG]^+$.
174x276mm (300 x 300 DPI)

Graphical Abstract

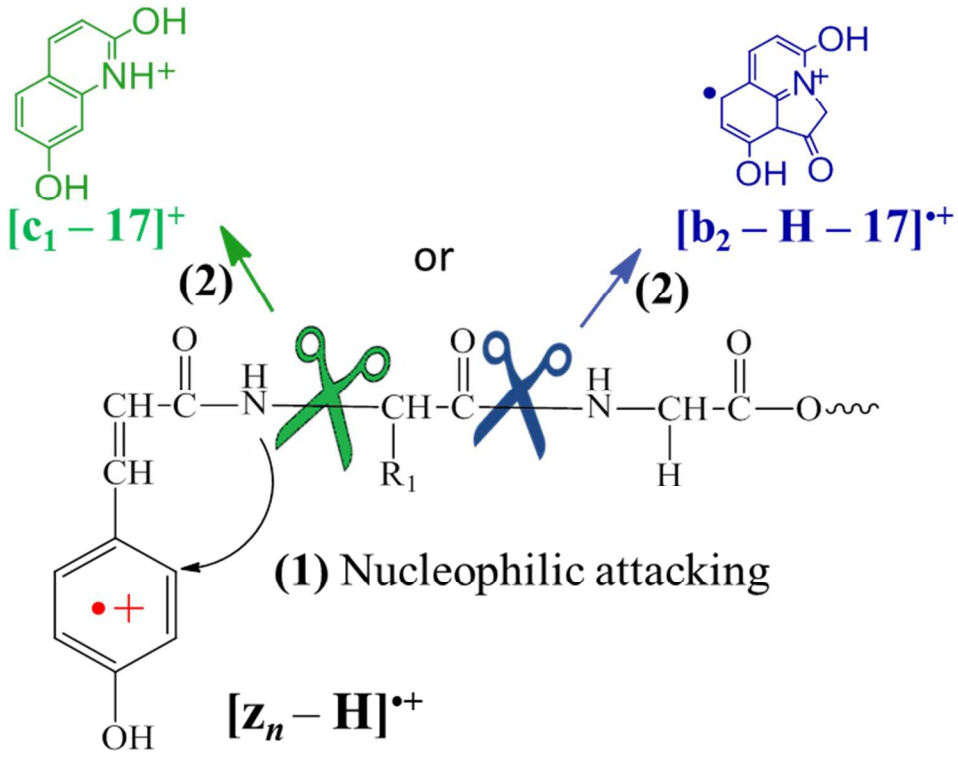

Residue-specific $[c_1 - 17]^+$ and $[b_2 - H - 17]^{\bullet+}$ fragment ions reveal a novel cyclic rearrangement between peptide backbones and sidechains.

Nucleophilic substitution by amide nitrogen in the aromatic rings of $[z_n - H]^{\bullet+}$ ions; the structures of the $[b_2 - H - 17]^{\bullet+}$ and $[c_1 - 17]^{+}$ ions

Xiaoyan Mu,[a] Justin Kai-Chi Lau,[b,c] Cheuk-Kuen Lai,[a] K.W. Michael Siu,[b,c] Alan C. Hopkinson,[b] Ivan K. Chu[a*]*

[a]*Department of Chemistry,The University of Hong Kong, Hong Kong, China.*
[b]*Department of Chemistry and Centre for Research in Mass Spectrometry, York University, 4700 Keele Street, Toronto ON, Canada M3J 1P3*
[c]*Department of Chemistry and Biochemistry, University of Windsor, 401 Sunset Avenue, Windsor, ON, Canada N9B 3P4*

Supplementary Materials

*Corresponding authors

Email: ach@yorku.ca; ivankchu@hku.hk

Scheme S1 Detailed mehcanism showing the formations of $[c_1 - 17]^+$ and $[b_2 - H - 17]^{\bullet+}$ ions from $[YGG]^{\bullet+}$ via nucleophilic attack by backbone nitrogen or oxygen. Upper numbers are the relative enthalpies (ΔH^o_0) and free energies (ΔG^o_{298}, in parenthesis) calculated at M062X/6-31++G(d,p) level while the lower numbers are those calculated at the B3LYP/6-31++G(d,p) level. All energies are in kcal mol^{-1}.

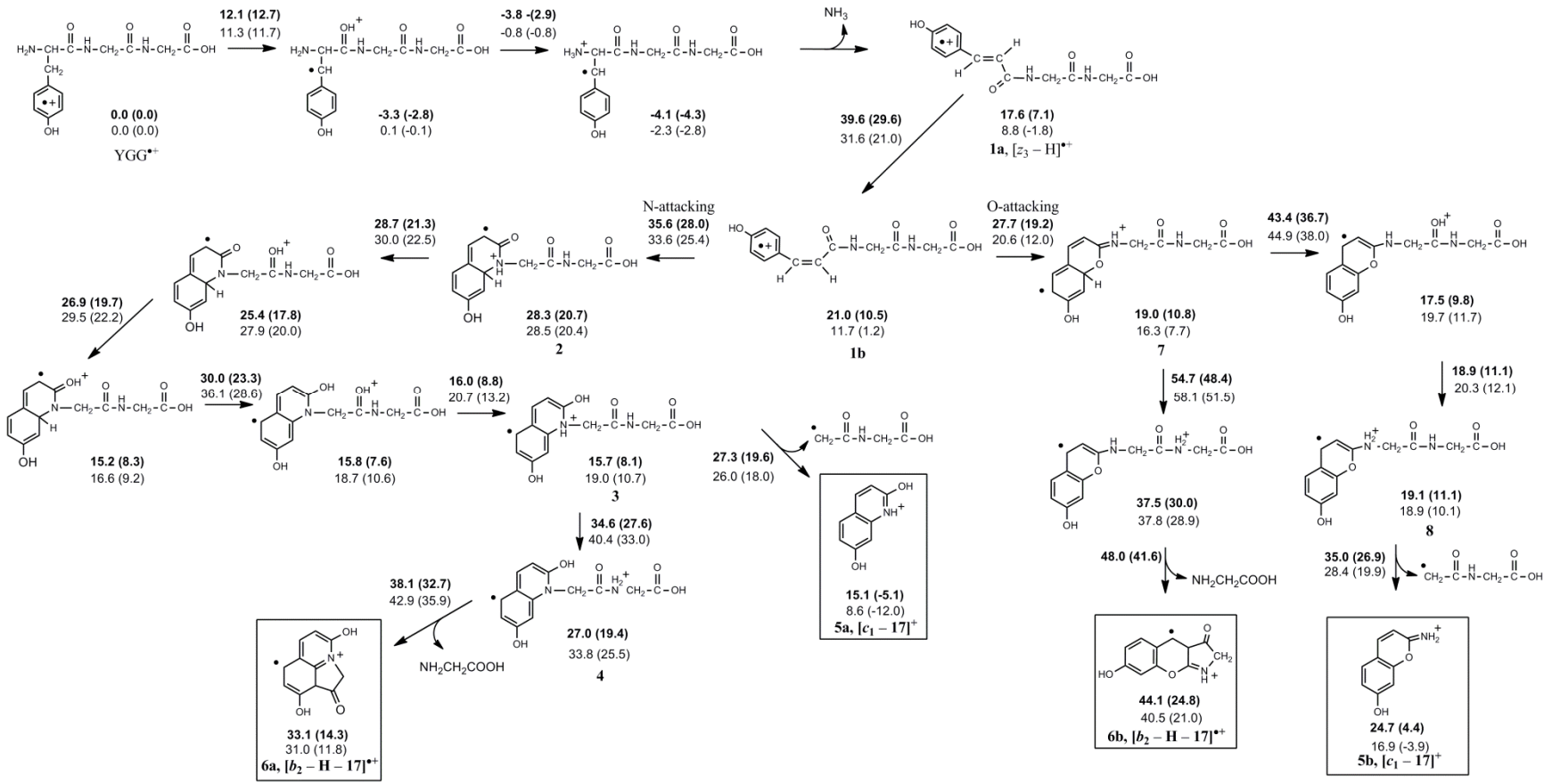

Figure S1. CID spectra of (a) $[Y_{\pi}^{\bullet}GGA]^{+}$ and (b) $[z_4 - H]^{\bullet+}$ generated from $[Y_{\pi}^{\bullet}GGA]^{+}$.

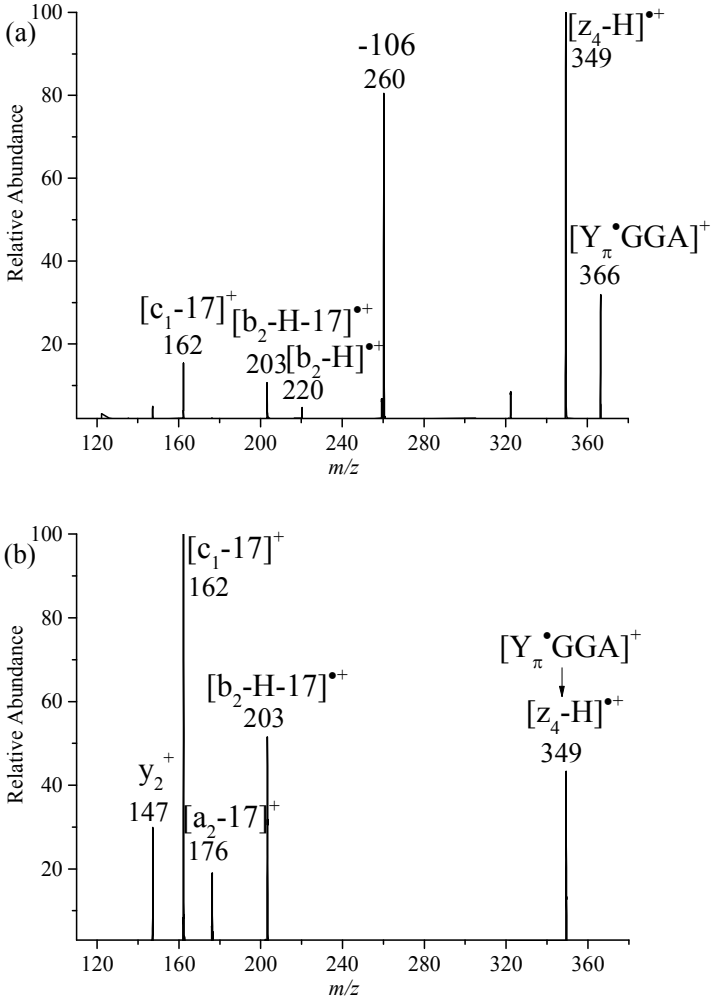

Figure S2 CID spectra of (a) $[Y_{\pi}^{\bullet}GG]^{+}$ and (b) $[z_3 - H]^{\bullet+}$ generated from $[Y_{\pi}^{\bullet}GG]^{+}$.

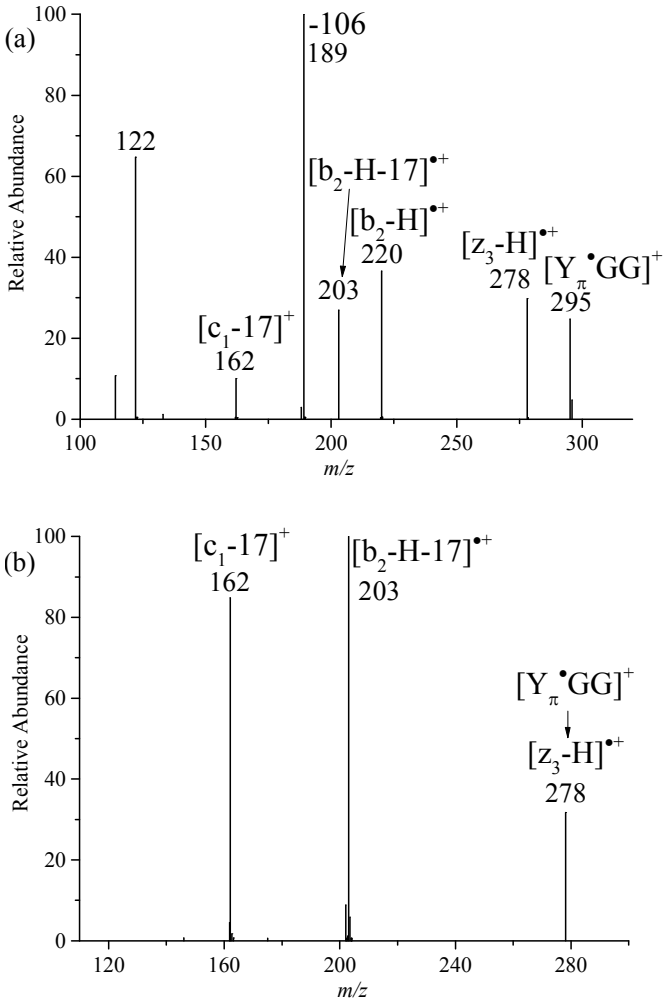

Figure S3 CID spectra of (a) $[c_1 - 17]^+$ and (b) $[b_2 - H - 17]^{\bullet+}$ generated from $[W_\pi^\bullet GG]^+$.

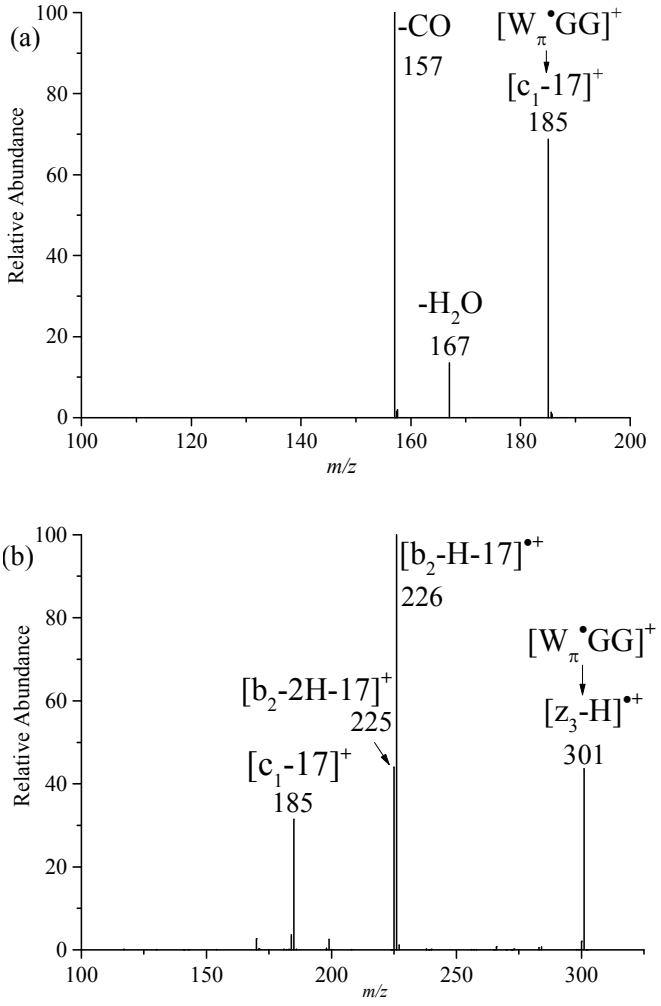

Figure S4 CID spectra of (a) $[F_\pi^{\bullet}GG]^+$, (b) $[z_3 - H]^{\bullet+}$ and (c) $[c_1 - 17]^+$ generated from $[F_\pi^{\bullet}GG]^+$.

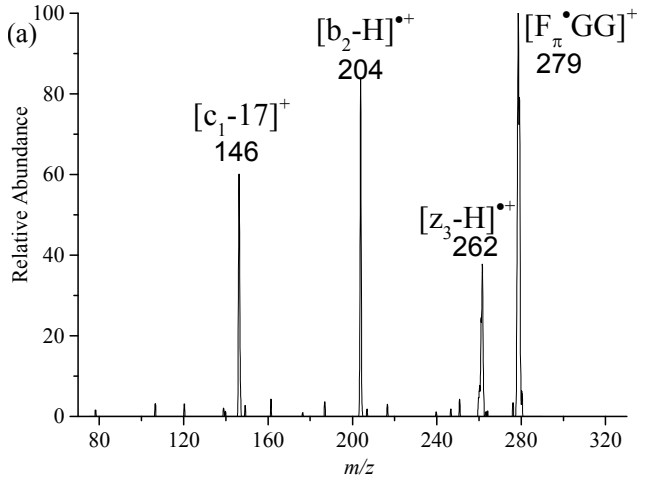

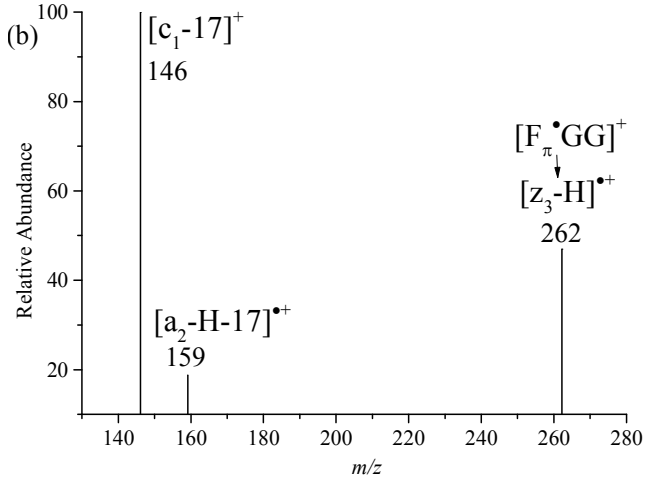

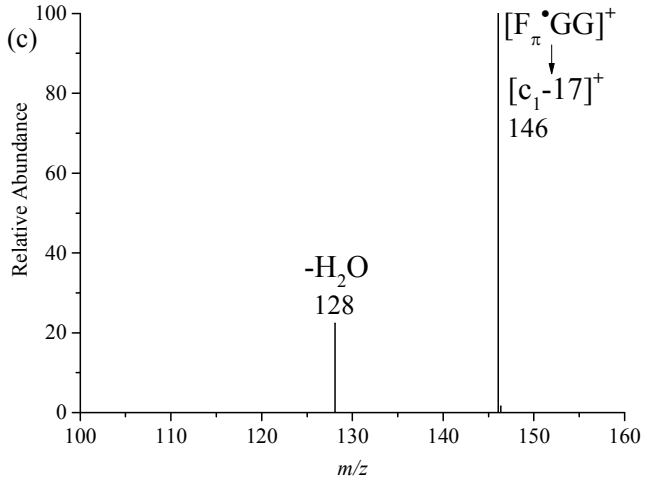

Figure S5. CID spectra of (a) $[F_{5D}GG_{\alpha}^{\bullet}]^+$, (b) $[c_1 - 17]^+$ generated from $[F_{5D}GG_{\alpha}^{\bullet}]^+$, (c) $[FG_{N15}G_{\alpha}^{\bullet}]^+$ and (d) $[c_1 - 17]^+$ generated from $[FG_{N15}G_{\alpha}^{\bullet}]^+$.

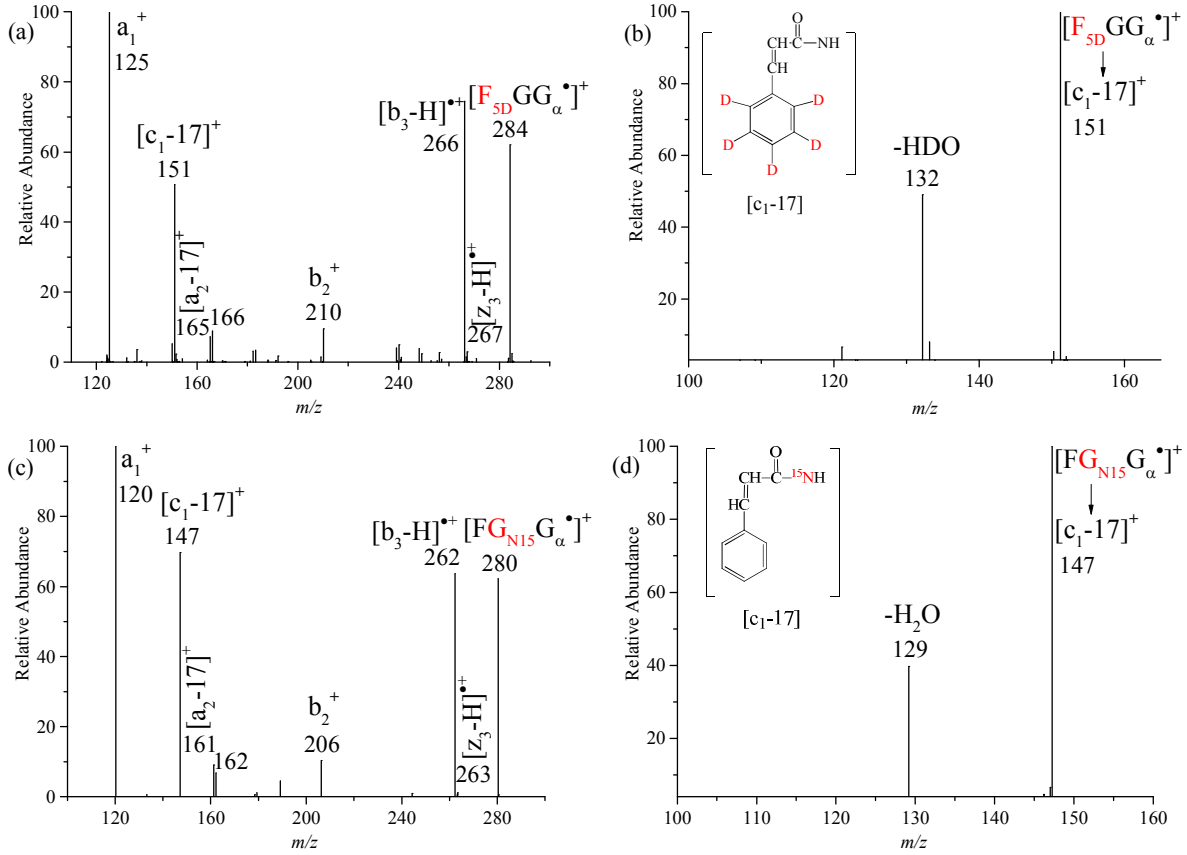

Figure S6 Nine optimized structures proposed for $[c_1\text{-}17]^+$. The relative enthalpies (ΔH^o_0) and free energies (ΔG^o_{298}, in parenthesis) are shown in kcal mol^{-1}.

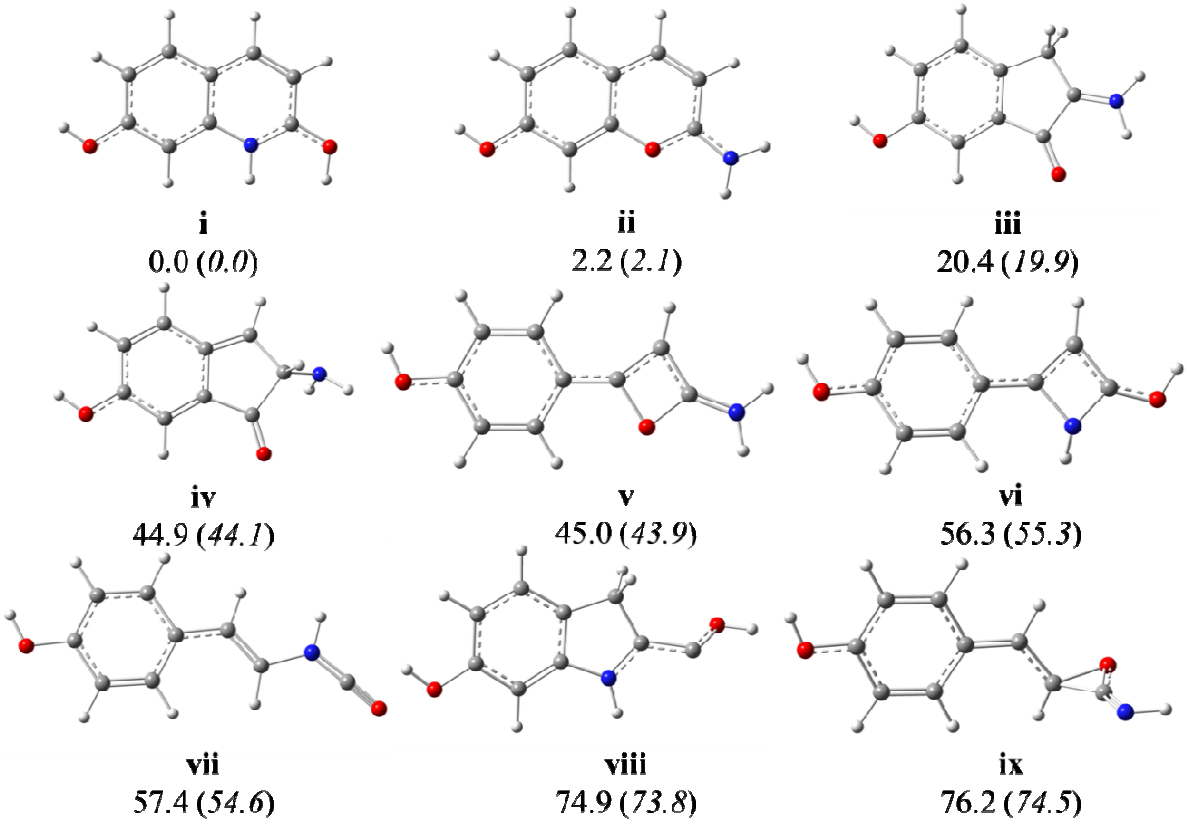

Figure S7 CID spectra of (a) protonated 2,7-dihydroxyquinoline and (b) quinolin-2(1H)-one.

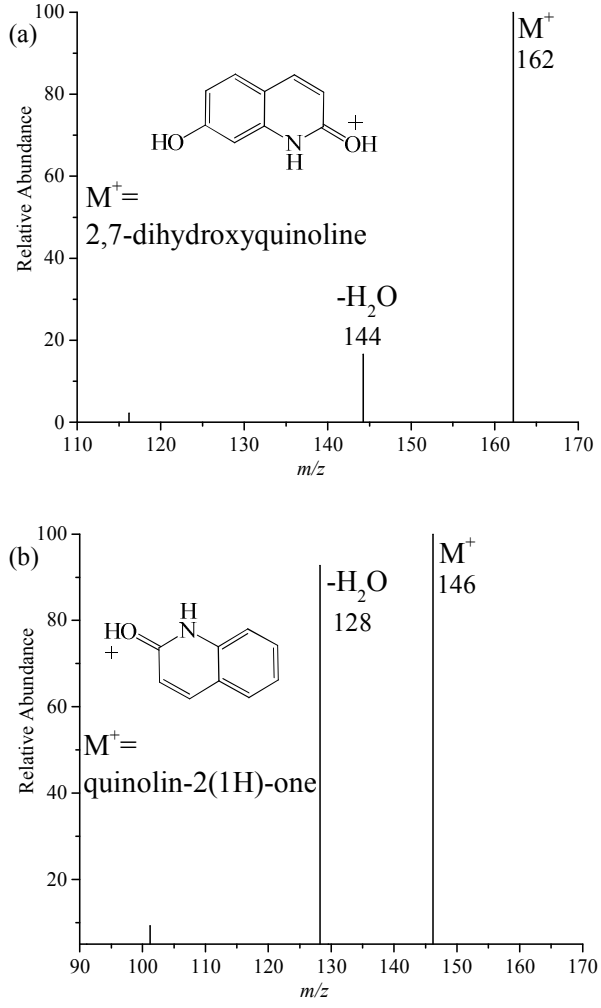

Figure S8 CID spectra mentioned in Table 1.

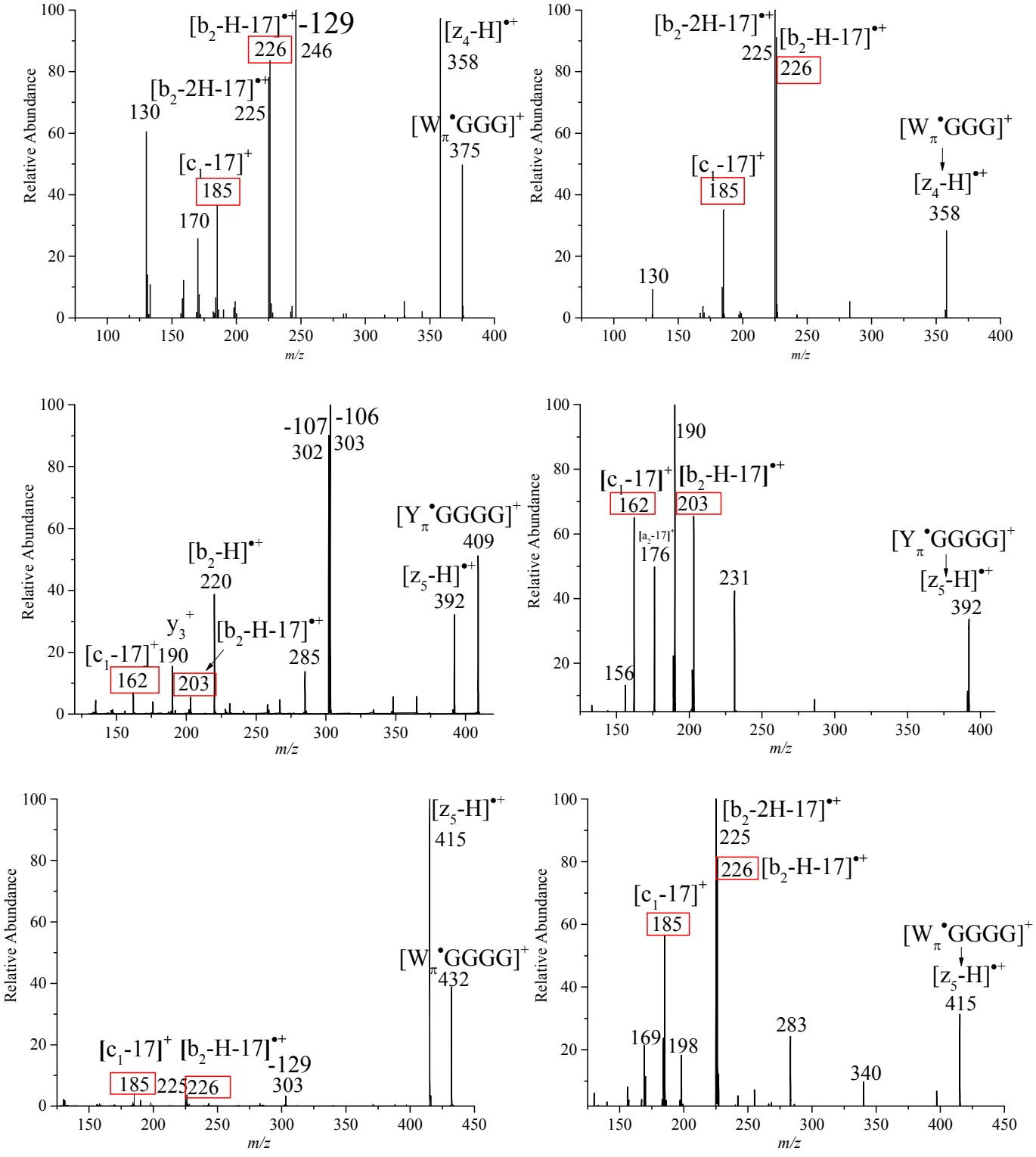

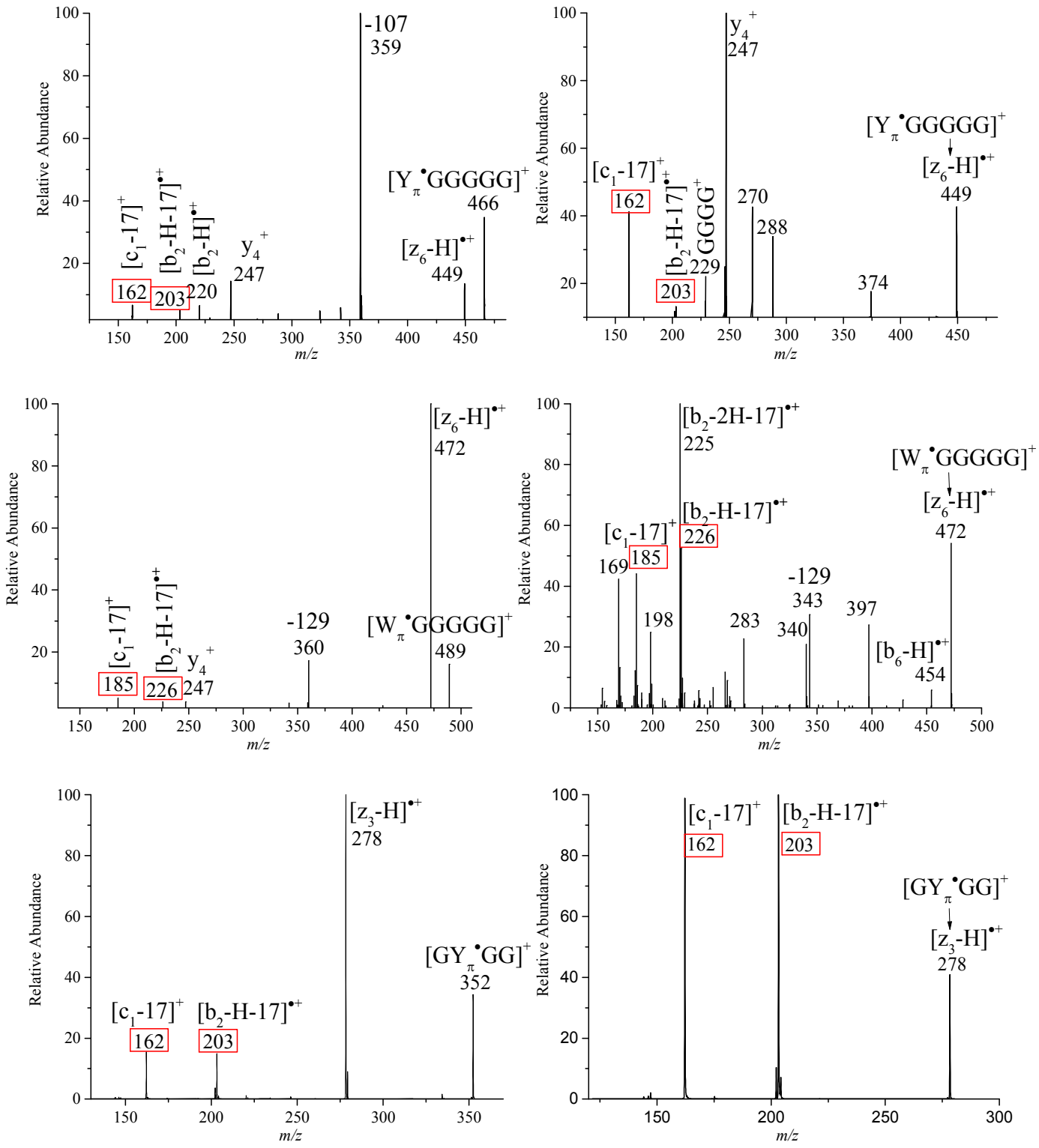
Relative Abundance
m/z
-107
359
[Y$_\pi^\bullet$GGGGG]$^+$
466
[z$_6$-H]$^{\bullet+}$
449
y$_4^+$
247
[c$_1$-17]$^+$
162
[b$_2$-H-17]$^{\bullet+}$
203
[b$_2$-H]$^{\bullet+}$
220
[c$_1$-17]$^+$
162
[b$_2$-H-17]$^{\bullet+}$
203
y$_4^+$
247
GGGGG
229
270
288
374
[Y$_\pi^\bullet$GGGGG]$^+$
[z$_6$-H]$^{\bullet+}$
449
[z$_6$-H]$^{\bullet+}$
472
[c$_1$-17]$^+$
185
[b$_2$-H-17]$^{\bullet+}$
226
y$_4^+$
247
-129
360
[W$_\pi^\bullet$GGGGG]$^+$
489
[b$_2$-2H-17]$^{\bullet+}$
225
[b$_2$-H-17]$^{\bullet+}$
226
[c$_1$-17]$^+$
169
185
198
283
-129
343
340
397
[b$_6$-H]$^{\bullet+}$
454
[W$_\pi^\bullet$GGGGG]$^+$
[z$_6$-H]$^{\bullet+}$
472
[z$_3$-H]$^{\bullet+}$
278
[GY$_\pi^\bullet$GG]$^+$
352
[c$_1$-17]$^+$
162
[b$_2$-H-17]$^{\bullet+}$
203
[c$_1$-17]$^+$
162
[b$_2$-H-17]$^{\bullet+}$
203
[GY$_\pi^\bullet$GG]$^+$
[z$_3$-H]$^{\bullet+}$
278

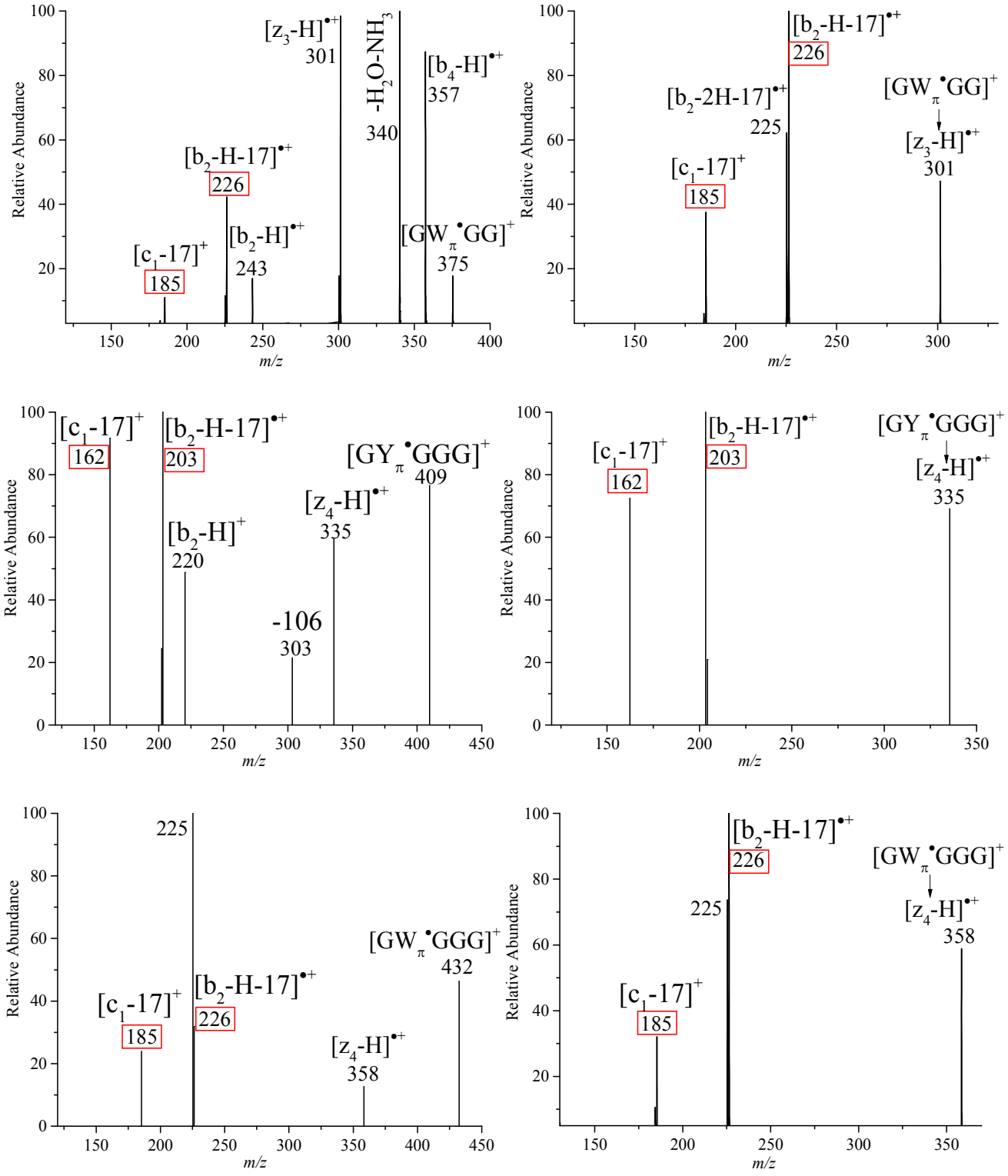
Relative Abundance
m/z
[z3-H]•+
301
-H2O-NH3
340
[b4-H]•+
357
[b2-H-17]•+
226
[b2-H]•+
243
[c1-17]+
185
[GWπ•GG]+
375
[b2-H-17]•+
226
[b2-2H-17]•+
225
[GWπ•GG]+
[z3-H]•+
301
[c1-17]+
185
[c1-17]+
162
[b2-H-17]•+
203
[GYπ•GGG]+
409
[z4-H]•+
335
[b2-H]+
220
-106
303
[c1-17]+
162
[b2-H-17]•+
203
[GYπ•GGG]+
[z4-H]•+
335
225
[GWπ•GGG]+
432
[c1-17]+
185
[b2-H-17]•+
226
[z4-H]•+
358
[b2-H-17]•+
226
[GWπ•GGG]+
[z4-H]•+
358
225
[c1-17]+
185

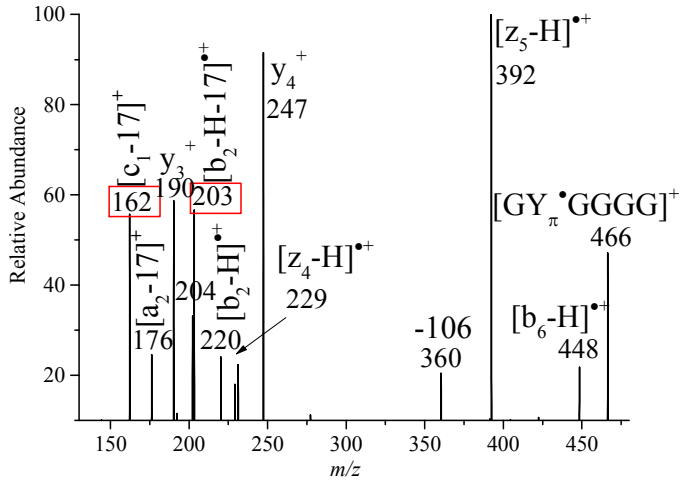
Relative Abundance
m/z
[c1-17]+
162
y3+
190
[b2-H-17]•+
203
y4+
247
[a2-17]+
176
204
[b2-H]•+
220
[z4-H]•+
229
-106
360
[z5-H]•+
392
[GYπ•GGGG]+
466
[b6-H]•+
448

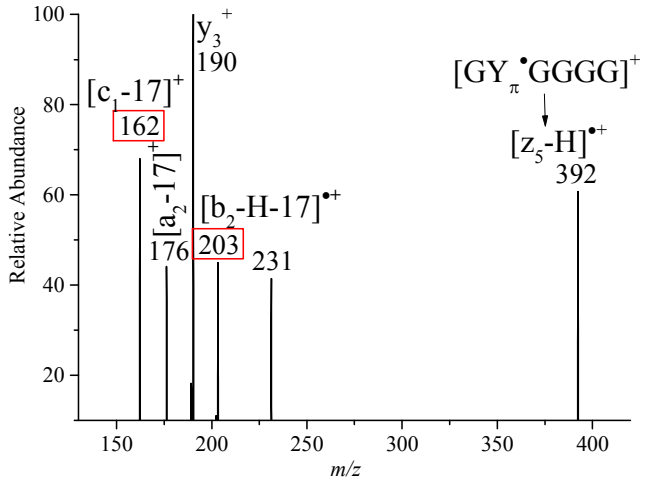
Relative Abundance
m/z
y3+
190
[c1-17]+
162
[a2-17]+
176
[b2-H-17]•+
203
231
[GYπ•GGGG]+
[z5-H]•+
392

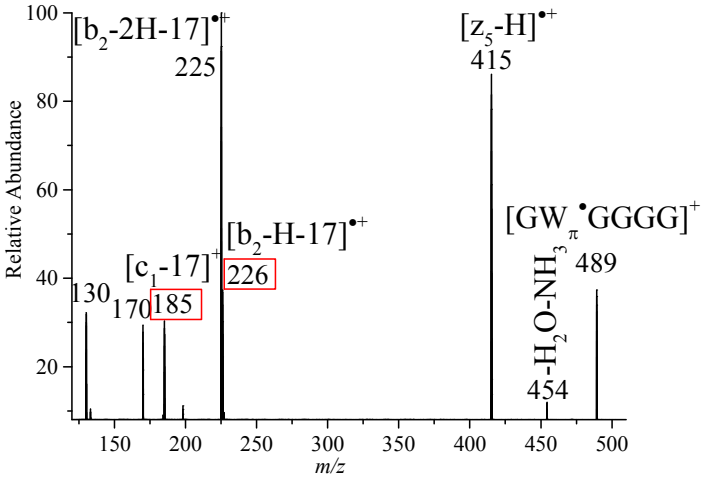
Relative Abundance
m/z
[b2-2H-17]•+
225
[z5-H]•+
415
[b2-H-17]•+
[c1-17]+
226
185
130
170
[GWπ•GGGG]+
489
-H2O-NH3
454

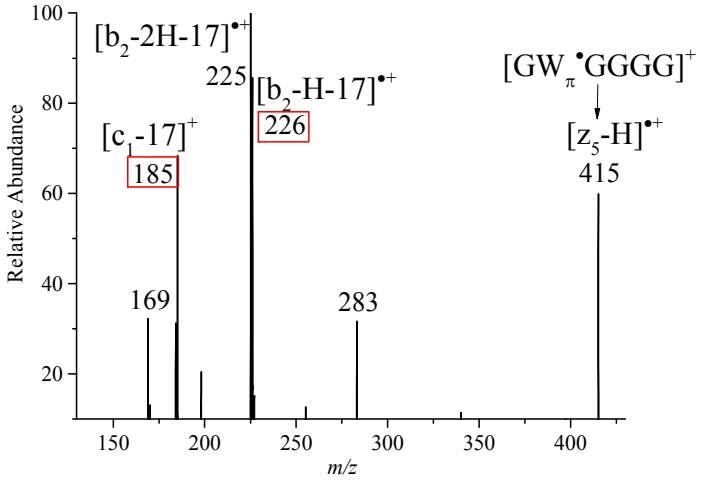
Relative Abundance
m/z
[b2-2H-17]•+
225
[b2-H-17]•+
226
[c1-17]+
185
169
283
[GWπ•GGGG]+
[z5-H]•+
415

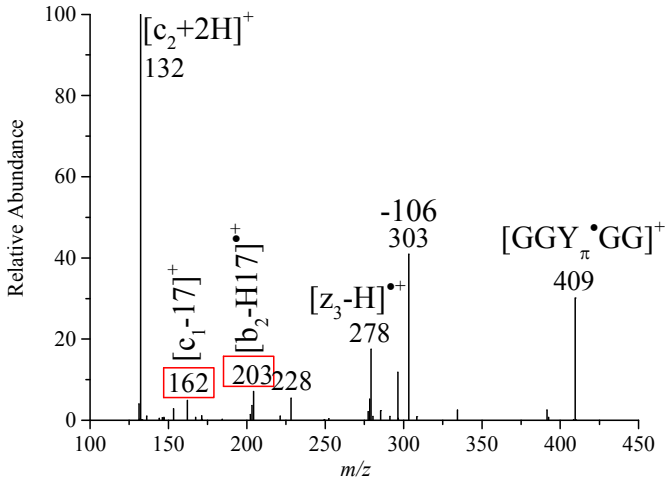
Relative Abundance
m/z
[c2+2H]+
132
[c1-17]+
162
[b2-H17]•+
203
228
[z3-H]•+
278
-106
303
[GGYπ•GG]+
409

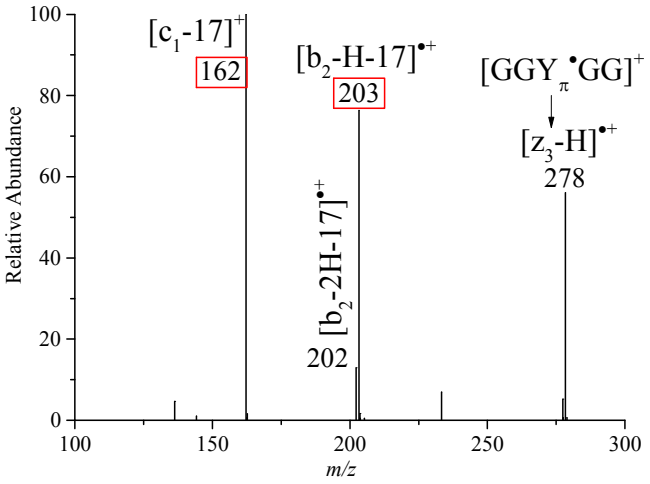
Relative Abundance
m/z
[c1-17]+
162
[b2-H-17]•+
203
[b2-2H-17]•+
202
[GGYπ•GG]+
[z3-H]•+
278

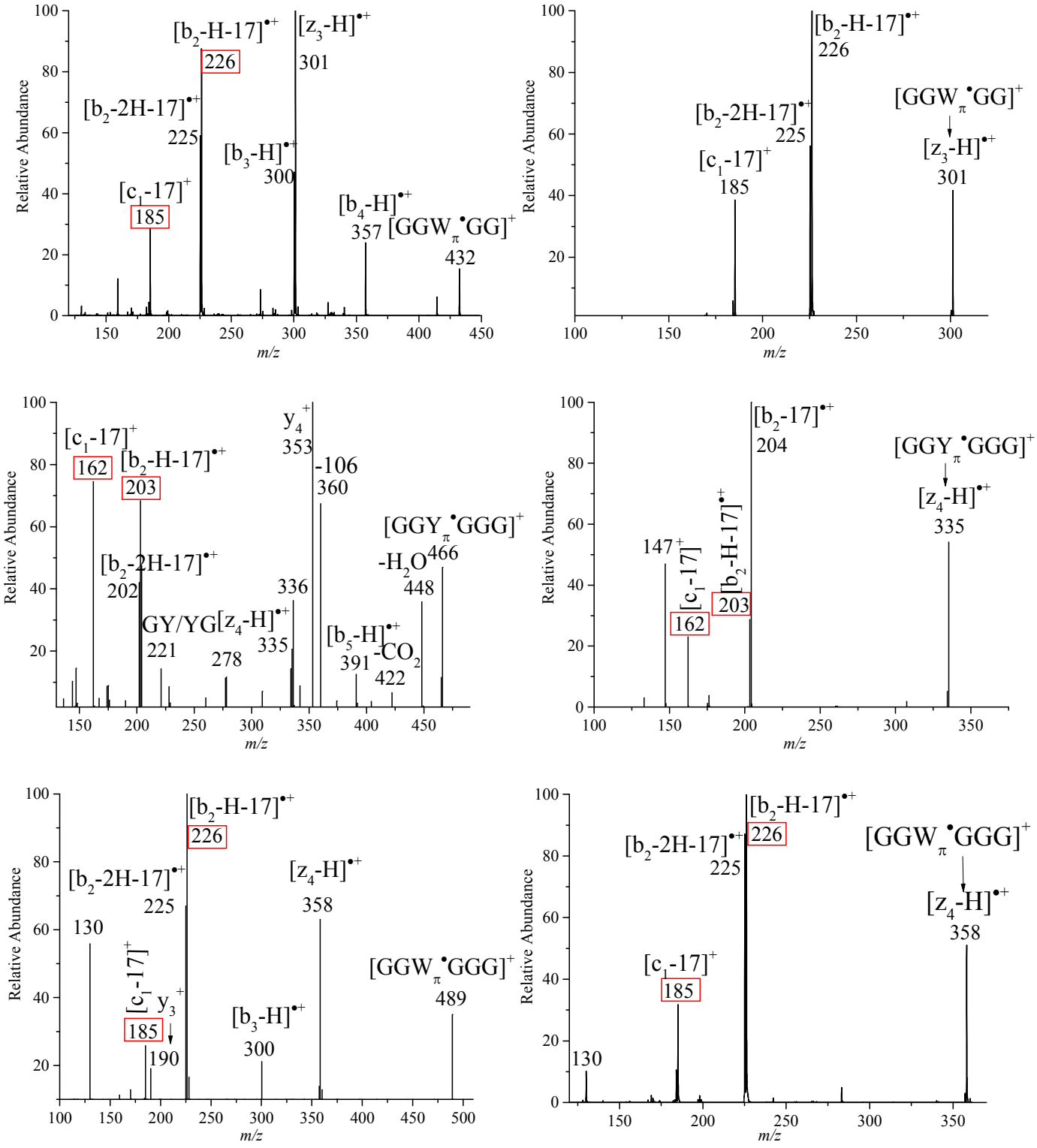
Relative Abundance
m/z
[b2-H-17]•+
226
[z3-H]•+
301
[b2-2H-17]•+
225
[b3-H]•+
300
[c1-17]+
185
[b4-H]•+
357
[GGWπ•GG]+
432
[GGWπ•GG]+
[z3-H]•+
301
[c1-17]+
185
[b2-2H-17]•+
225
[c1-17]+
162
[b2-H-17]•+
203
y4+
353
-106
360
[GGYπ•GGG]+
-H2O
466
448
[b2-2H-17]•+
202
GY/YG
221
278
[z4-H]•+
335
336
[b5-H]•+
-CO2
391
422
[b2-17]•+
204
[GGYπ•GGG]+
[z4-H]•+
335
147+
[c1-17]
162
[b2-H-17]+
203
[b2-H-17]•+
226
[b2-2H-17]•+
225
130
[c1-17]+
y3+
185
190
[z4-H]•+
358
[b3-H]•+
300
[GGWπ•GGG]+
489
[b2-H-17]•+
226
[b2-2H-17]•+
225
[GGWπ•GGG]+
[z4-H]•+
358
[c1-17]+
185
130

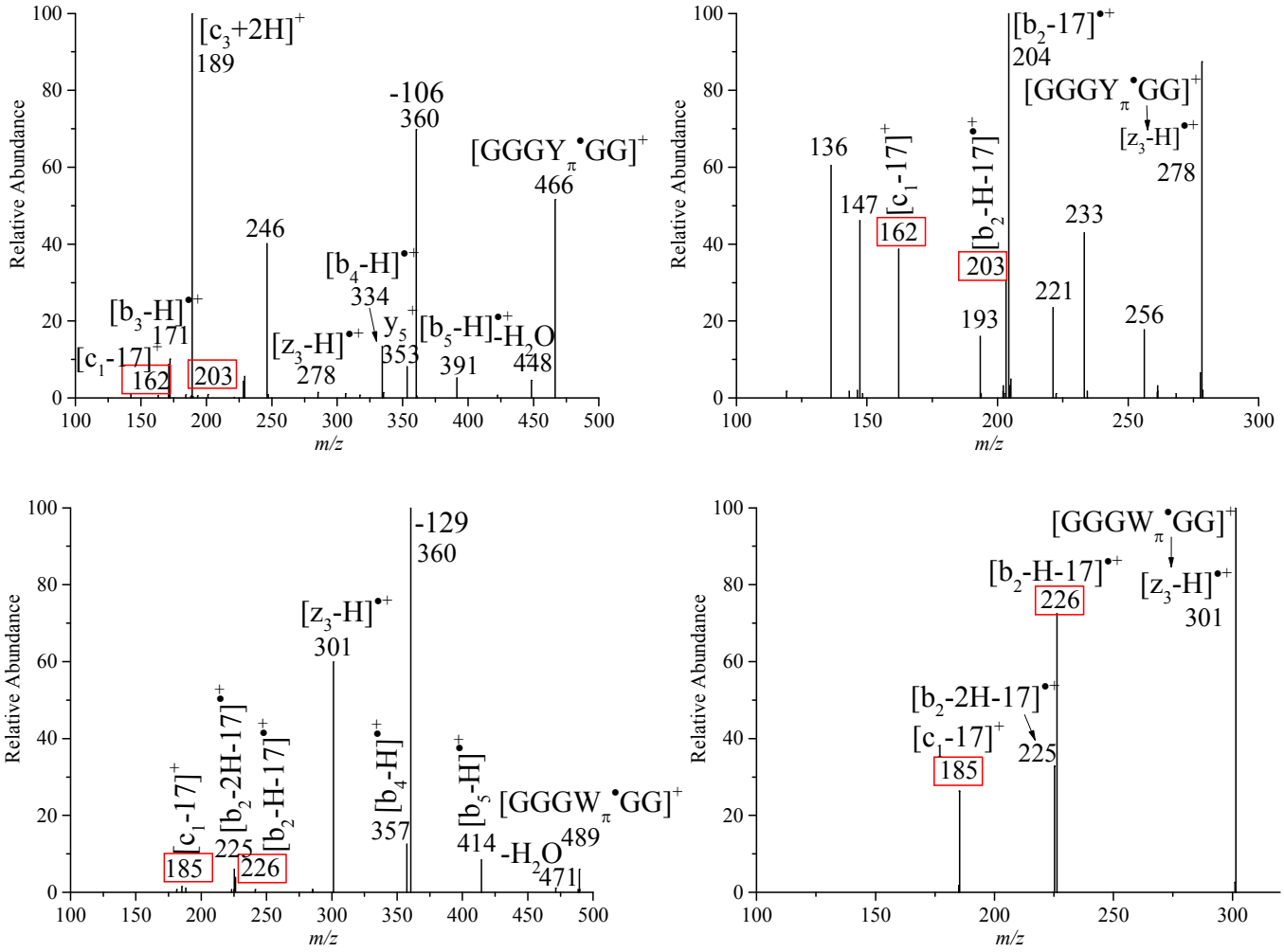
Relative Abundance
m/z
[c3+2H]+
189
-106
360
[GGGYπ•GG]+
466
246
[b4-H]•+
334
[b3-H]•+
171
[c1-17]+
162
203
[z3-H]•+
278
y5+
353
[b5-H]•+
391
-H2O
448
[b2-17]•+
204
[GGGYπ•GG]+
[z3-H]•+
278
136
147
[c1-17]+
162
[b2-H-17]•+
203
233
221
193
256
-129
360
[z3-H]•+
301
[c1-17]+
185
[b2-2H-17]•+
225
[b2-H-17]•+
226
[b4-H]•+
357
[b5-H]•+
414
-H2O
489
[GGGWπ•GG]+
471
[GGGWπ•GG]+
[b2-H-17]•+
226
[z3-H]•+
301
[b2-2H-17]•+
[c1-17]+
225
185

Figure S9 CID spectra of $[Y_{\pi}^{\bullet}AG]^{+}$, $[Y_{\pi}^{\bullet}VG]^{+}$,$[Y_{\pi}^{\bullet}LG]^{+}$,$[Y_{\pi}^{\bullet}PG]^{+}$ and their $[z_3\text{-H}]^{\bullet+}$.

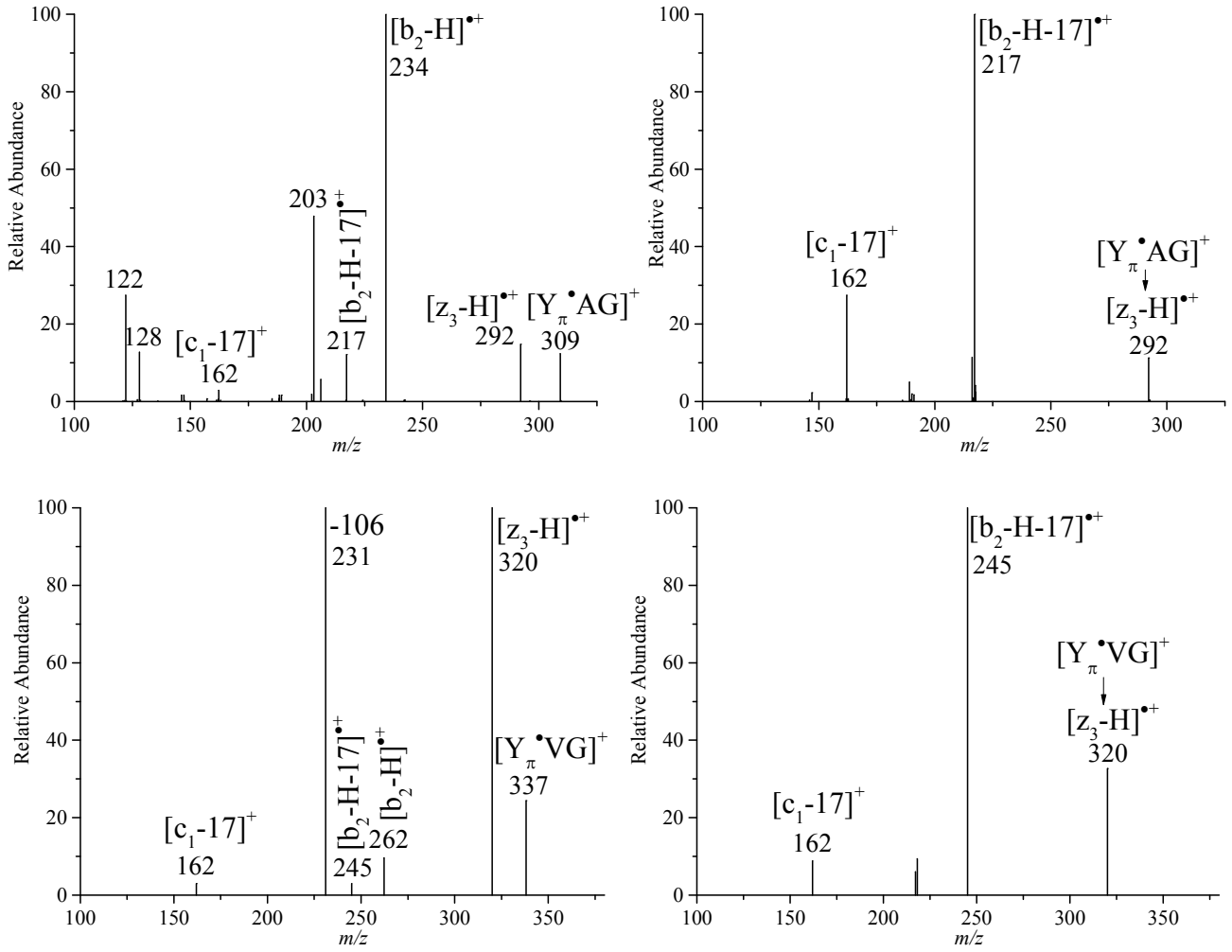

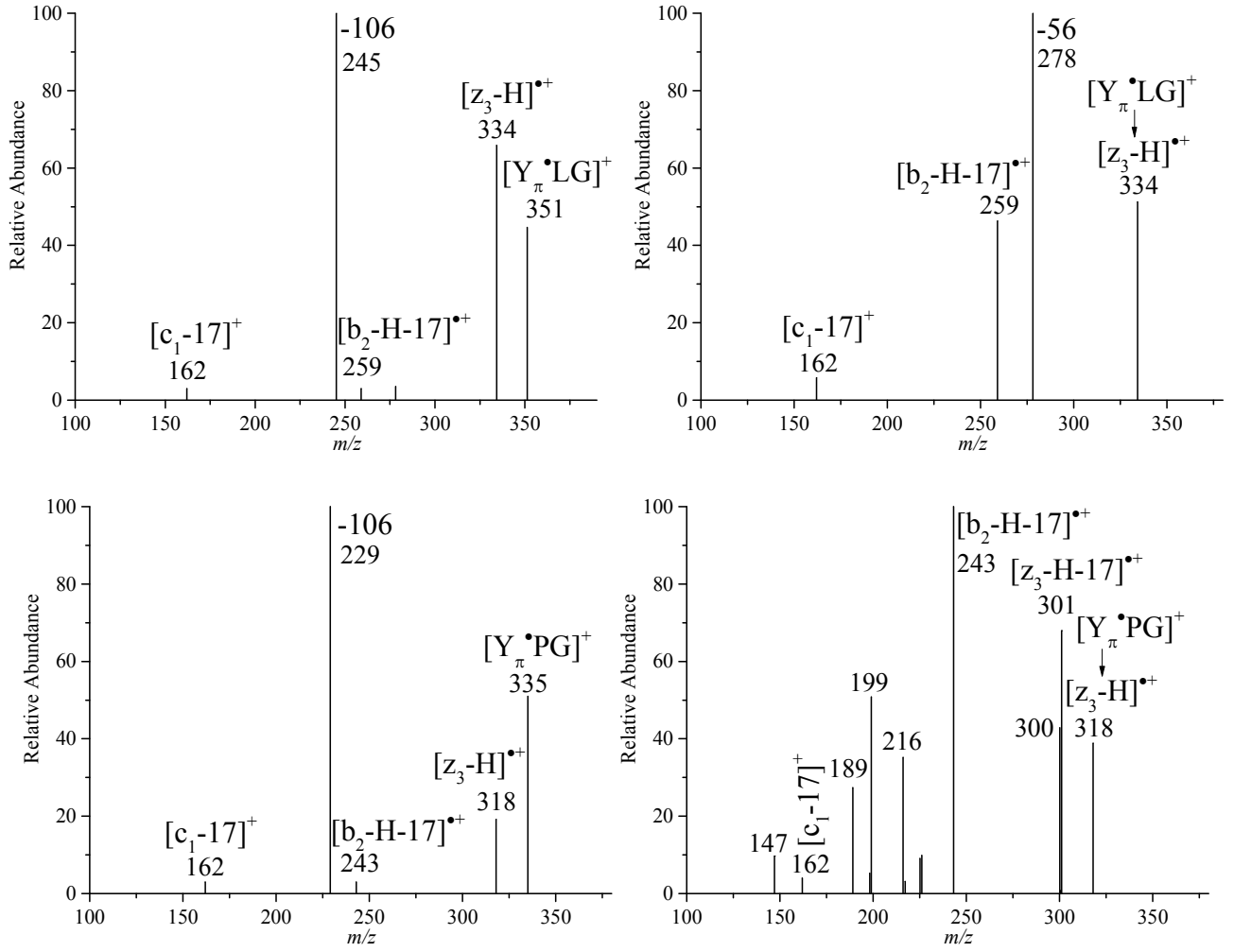
Relative Abundance
m/z
-106
245
[z3-H]•+
334
[Yπ•LG]+
351
[c1-17]+
162
[b2-H-17]•+
259
-56
278
[Yπ•LG]+
[z3-H]•+
334
[b2-H-17]•+
259
[c1-17]+
162
-106
229
[Yπ•PG]+
335
[z3-H]•+
318
[c1-17]+
162
[b2-H-17]•+
243
[b2-H-17]•+
243
[z3-H-17]•+
301
[Yπ•PG]+
[z3-H]•+
318
199
216
189
[c1-17]+
147
162
300

Cartesian coordinate of selected structures optimized at the M06-2X/6-31++G(d,p) level

Structure_1a.xyz

34

C	1.512709	0.169518	0.000028
C	0.233234	0.954660	0.000042
O	0.254281	2.177675	0.000032
H	1.470383	-0.916413	0.000026
C	2.692705	0.870246	0.000015
C	3.997602	0.316945	-0.000003
H	2.589488	1.954998	0.000016
C	6.628241	-0.638740	-0.000042
C	5.110273	1.220462	-0.000025
C	4.264134	-1.092688	-0.000002
C	5.543711	-1.562615	-0.000022
C	6.398057	0.763235	-0.000045
H	4.912372	2.288105	-0.000027
H	3.441846	-1.799329	0.000017
H	5.773850	-2.622296	-0.000020
H	7.238425	1.451158	-0.000063
N	-0.884803	0.210368	0.000063
C	-2.191245	0.824240	0.000069
C	-3.215117	-0.309334	0.000078
O	-2.852267	-1.480356	0.000086
H	-0.892704	-0.807244	0.000068
H	-2.315190	1.461172	0.883918
H	-2.315198	1.461169	-0.883781
N	-4.503444	0.066602	0.000079
C	-5.563448	-0.915551	0.000057
C	-6.885139	-0.183011	-0.000080
O	-6.989602	1.019299	-0.000158
O	-7.913515	-1.030629	-0.000098
H	-4.785513	1.041330	0.000038
H	-5.507107	-1.564052	0.881086
H	-8.738592	-0.518899	-0.000183
H	-5.506969	-1.564149	-0.880893
O	7.833175	-1.162095	-0.000057
H	8.541762	-0.499685	-0.000062

Structure_1b.xyz

```
 34

C    1.434128   1.558674   0.081338
C    0.513370   0.378559   0.125272
O    0.875454  -0.792791   0.168774
C    2.806609   1.650973   0.018848
C    3.873659   0.704305  -0.003154
H    3.154379   2.681082  -0.031008
C    6.151067  -0.931531  -0.072047
C    3.752249  -0.723083   0.101407
C    5.193336   1.265880  -0.134665
C    6.307095   0.480314  -0.172864
C    4.862524  -1.516777   0.066855
H    2.762752  -1.152635   0.205418
H    5.297983   2.344082  -0.209349
H    7.297726   0.913023  -0.277457
H    4.796606  -2.596461   0.145013
N   -0.781644   0.739552   0.109476
C   -1.835221  -0.246053   0.130818
C   -3.156423   0.518558   0.048565
O   -3.165380   1.742784  -0.005710
H   -1.108638   1.702984   0.065539
H   -1.728907  -0.937204  -0.713624
H   -1.786348  -0.841048   1.050510
N   -4.268579  -0.232075   0.040987
C   -5.575205   0.380069  -0.044461
C   -6.608910  -0.721109  -0.088792
O   -6.341908  -1.897614  -0.048382
O   -7.843790  -0.228947  -0.176090
H   -4.242186  -1.245698   0.077181
H   -5.664078   1.002009  -0.941720
H   -8.472925  -0.968016  -0.198071
H   -5.771411   1.027884   0.816959
H    0.924533   2.519871   0.085316
O    7.170052  -1.758590  -0.098474
H    8.026980  -1.313626  -0.191596

Structure_2.xyz
 34

C    3.359631  -2.169245   0.238351
```

```
C    1.975230   -2.384764   -0.108452
O    1.409205   -3.412919   -0.329770
C    3.876697   -0.920325    0.424517
C    3.148279    0.259633    0.116667
H    4.882997   -0.816146    0.822340
C    1.506939    2.532238   -0.324812
C    1.873671    0.099890   -0.666305
C    3.587135    1.528500    0.484818
C    2.806541    2.653571    0.276405
C    1.032771    1.328748   -0.741615
H    2.134516   -0.236518   -1.687372
H    4.547262    1.626540    0.983044
H    3.161759    3.629395    0.593117
H    0.070660    1.301418   -1.241927
N    1.112180   -1.091477   -0.088317
C   -0.239166   -1.298676   -0.668502
C   -1.217109   -0.633314    0.306937
O   -0.809053   -0.320874    1.422881
H    0.892664   -0.853069    0.911868
H   -0.282684   -0.891399   -1.680676
H   -0.426270   -2.374764   -0.708163
N   -2.465758   -0.458416   -0.121880
C   -3.491630    0.089539    0.744441
C   -4.794753    0.070761   -0.025571
O   -4.891880   -0.343320   -1.155057
O   -5.794474    0.562167    0.697658
H   -2.775772   -0.760153   -1.042055
H   -3.252955    1.116206    1.040201
H   -6.612777    0.527241    0.175258
H   -3.593860   -0.502232    1.659967
H    3.934957   -3.072122    0.404524
O    0.724095    3.613783   -0.499408
H    1.145985    4.424806   -0.190445


Structure_3.xyz
 34


C    2.978076   -2.353670    0.442016
C    1.822557   -2.302317   -0.276121
O    1.119306   -3.282431   -0.865882
C    3.566402   -1.183485    0.947050
```

```
C    3.015799   0.087793   0.595361
H    4.476684  -1.235023   1.530701
C    1.970147   2.547776  -0.322317
C    1.827355   0.170762  -0.151155
C    3.654355   1.311251   0.885107
C    3.145294   2.518103   0.443798
C    1.296578   1.357982  -0.619573
H    0.624761  -1.015102  -1.342424
H    4.575720   1.293804   1.458873
H    3.661941   3.444087   0.679013
H    0.390630   1.393307  -1.216396
N    1.044320  -1.069234  -0.382442
C   -0.198605  -1.128998   0.489657
C   -1.344005  -0.598941  -0.380722
O   -1.155032  -0.476027  -1.588798
H    1.604868  -4.118838  -0.877197
H   -0.385025  -2.175155   0.743914
H   -0.017160  -0.540565   1.390173
N   -2.490588  -0.329885   0.239049
C   -3.660278   0.111872  -0.496437
C   -4.782379   0.297921   0.502445
O   -4.657245   0.095144   1.685624
O   -5.898025   0.706320  -0.090737
H   -2.609930  -0.437121   1.243143
H   -3.954645  -0.624423  -1.251374
H   -6.595105   0.812555   0.577507
H   -3.467798   1.056775  -1.014814
H    3.453617  -3.318850   0.584238
O    1.423958   3.680298  -0.800299
H    1.953845   4.455672  -0.575528


Structure_4.xyz
 34


C   -1.284439   2.918139  -0.157847
C   -0.275001   2.081649   0.214031
O    1.069155   2.377194   0.258989
C   -2.587876   2.415198  -0.308015
C   -2.811372   1.004413  -0.209421
H   -3.409445   3.075135  -0.555337
C   -3.164815  -1.794008  -0.068598
```

```
C   -1.741191   0.141033   0.138690
C   -4.057723   0.403249  -0.464408
C   -4.243084  -0.969076  -0.394740
C   -1.909096  -1.237156   0.197057
H    1.030835  -0.325758  -1.412944
H   -4.896382   1.043000  -0.721464
H   -5.220348  -1.400177  -0.591675
H   -1.107867  -1.920410   0.462216
N   -0.476287   0.714397   0.443464
C    0.405661   0.018214   1.354058
C    1.386810  -0.851949   0.603192
O    1.855299  -1.901065   0.871437
H    1.216063   3.327820   0.349592
H    1.005920   0.732525   1.930169
H   -0.149589  -0.619648   2.047113
N    1.805537  -0.200561  -0.749250
C    3.079787  -0.760742  -1.263442
C    4.163345  -0.311851  -0.296601
O    3.920394   0.416466   0.633938
O    5.340927  -0.807423  -0.625639
H    1.886406   0.820972  -0.570133
H    3.270862  -0.374332  -2.266917
H    6.016936  -0.509493   0.007310
H    3.015040  -1.849916  -1.293451
H   -1.058591   3.958806  -0.367579
O   -3.250822  -3.142006   0.014106
H   -4.150245  -3.443385  -0.162778


Structure_5a.xyz
 20


C   -2.384225  -1.094736   0.000000
C   -2.397554   0.308472   0.000000
O   -3.472170   1.076088   0.000000
C   -1.163119  -1.731151   0.000000
C    0.050909  -1.010408   0.000000
H   -1.128217  -2.817257   0.000000
C    2.383270   0.545916   0.000000
C    0.000000   0.406508   0.000000
C    1.327452  -1.628092   0.000000
C    2.468948  -0.871935   0.000000
```

```
C     1.152115    1.188648    0.000000
H    -1.324007    2.010420    0.000000
H     1.388120   -2.711915    0.000000
H     3.444640   -1.348779    0.000000
H     1.116919    2.272860    0.000000
N    -1.251478    0.995242    0.000000
H    -4.296645    0.568916    0.000000
H    -3.319441   -1.641440    0.000000
O     3.467626    1.324696    0.000000
H     4.288558    0.814901    0.000000
```

Structure_5b.xyz

```
  20

C    -2.410885    1.012991    0.000000
C    -2.347707   -0.400706    0.000000
C    -1.233606    1.709219    0.000000
C     0.017497    1.037250    0.000000
H    -1.249805    2.795821    0.000000
C     2.379554   -0.468631    0.000000
C     0.010037   -0.369268    0.000000
C     1.274376    1.680103    0.000000
C     2.436245    0.944554    0.000000
C     1.154342   -1.139062    0.000000
H    -3.280369   -2.205536    0.000000
H     1.313505    2.764996    0.000000
H     3.400689    1.443284    0.000000
H     1.116178   -2.221787    0.000000
H    -3.378291    1.498743    0.000000
N    -3.401238   -1.200730    0.000000
H    -4.338002   -0.823811    0.000000
O    -1.192067   -1.039133    0.000000
O     3.474344   -1.232724    0.000000
H     4.287428   -0.710436    0.000000
```

Structure_6a.xyz

```
  24

C     2.707158    1.127464   -0.110077
C     2.413808   -0.243756   -0.056636
O     3.261339   -1.256575   -0.199926
```

C 1.687072 2.059445 -0.043046

C 0.337687 1.657427 0.128254

H 1.925795 3.114108 -0.146153

C -2.266615 0.463251 -0.025393

C 0.149284 0.295192 0.302064

C -0.848414 2.455787 0.003443

C -2.093080 1.828437 -0.163034

C -1.154631 -0.356347 0.562962

H -0.762301 3.531236 -0.092043

H -2.961538 2.416550 -0.441071

H -1.324123 -0.451322 1.657722

N 1.140545 -0.618840 0.145758

C 0.626701 -2.004749 0.080998

C -0.897171 -1.780042 0.071492

O -1.727328 -2.578843 -0.254801

H 4.165190 -0.960338 -0.378128

H 0.982214 -2.503284 -0.823217

H 0.933653 -2.579197 0.960364

H 3.736840 1.438122 -0.249174

O -3.441996 -0.114908 -0.267372

H -3.386464 -1.084037 -0.237971

Structure_6b.xyz

24

C 1.655596 0.459278 0.538333

C 1.323863 -0.930038 0.123440

C 0.603093 1.401519 0.057391

C -0.705958 0.898155 -0.018428

H 0.840572 2.450828 -0.066869

C -3.316584 -0.216339 -0.019474

C -0.961085 -0.494571 0.073646

C -1.864246 1.710877 -0.160265

C -3.132762 1.172699 -0.155064

C -2.205265 -1.067896 0.079113

H -1.731781 2.784224 -0.251516

H -3.997031 1.823491 -0.249545

H -2.339643 -2.142044 0.135632

H 1.732622 0.467001 1.646645

N 2.374155 -1.632620 -0.208308

H 2.303581 -2.586942 -0.551071

```
C    3.625023   -0.855814   -0.194721
H    4.281959   -1.169398    0.622088
H    4.148760   -0.944503   -1.148531
C    3.105530    0.576050    0.035507
O    3.718349    1.582445   -0.137154
O    0.129326   -1.404517    0.039293
O   -4.520507   -0.804664    0.003460
H   -5.238691   -0.163946   -0.080341
```

```
Structure_7.xyz
 34

C   -1.784402   -2.401450    0.126078
C   -0.959792   -1.227144    0.174628
C   -3.131076   -2.245357   -0.062363
C   -3.717719   -0.958906    0.013608
H   -3.748060   -3.105389   -0.308674
C   -4.578373    1.743247   -0.063581
C   -2.873512    0.108381    0.636993
C   -5.010278   -0.652506   -0.399891
C   -5.452820    0.662312   -0.427191
C   -3.318667    1.501204    0.389184
H   -2.856521   -0.076225    1.729291
H   -5.661720   -1.448242   -0.749242
H   -6.457785    0.885897   -0.773359
H   -2.669838    2.320707    0.677445
H   -1.297385   -3.368067    0.089188
N    0.345103   -1.284009    0.071968
H    0.832206   -2.177686   -0.042900
C    1.234905   -0.136903    0.070435
H    1.010552    0.522444   -0.774494
H    1.122288    0.435036    0.997184
C    2.651893   -0.713193   -0.052740
O    2.809773   -1.923188   -0.158942
N    3.648471    0.178069   -0.037917
H    3.490525    1.176361    0.060325
C    5.029398   -0.243153   -0.146779
C    5.896647    0.992783   -0.057029
H    5.296275   -0.938886    0.655638
H    5.216537   -0.754058   -1.097271
O    5.456327    2.109159    0.075335
```

O 7.188657 0.690105 -0.141474

H 7.708392 1.507815 -0.075492

O -1.470222 -0.014482 0.235120

O -4.982356 3.024585 -0.172903

H -5.875151 3.096550 -0.531204

Structure_8.xyz

34

C -1.872271 -2.491412 -0.228585

C -1.059818 -1.484764 0.208538

C -3.208424 -2.193013 -0.506449

C -3.654199 -0.842980 -0.330285

H -3.893665 -2.959333 -0.844988

C -4.409943 1.845213 0.057906

C -2.746345 0.140265 0.118602

C -4.970507 -0.412511 -0.578652

C -5.349186 0.904810 -0.391576

C -3.091063 1.459957 0.316811

H 0.597668 -1.254646 1.462714

H -5.699000 -1.138485 -0.926344

H -6.371586 1.212038 -0.590847

H -2.368130 2.185304 0.671212

H -1.476590 -3.495221 -0.345673

N 0.353143 -1.616938 0.511902

H 0.599489 -2.611206 0.528038

C 1.284804 -0.865781 -0.402376

H 1.531918 -1.490794 -1.261525

H 0.755721 0.031177 -0.732525

C 2.491917 -0.486525 0.465142

O 2.386426 -0.596297 1.683598

N 3.571166 -0.038602 -0.171903

H 3.624416 0.027339 -1.185281

C 4.749588 0.400240 0.551866

C 5.782414 0.812470 -0.475615

H 4.520803 1.247513 1.206537

H 5.149562 -0.403057 1.178875

O 5.587207 0.764098 -1.665866

O 6.904792 1.225381 0.100188

H 7.541284 1.480926 -0.587927

O -1.424123 -0.195724 0.387178

```
O   -4.707935   3.141874   0.263476
H   -5.634778   3.326771   0.067183
```

TS_1a-1b.xyz

```
 34

C    1.517006  -1.381685  -0.391418
C    0.484769  -0.583097   0.306593
O    0.803616   0.100829   1.278430
H    1.320795  -1.966068  -1.286777
C    2.798492  -1.503226   0.298739
C    3.891446  -0.702348   0.101972
H    2.875929  -2.285210   1.060741
C    6.127081   0.930972  -0.214301
C    5.085544  -0.933601   0.873450
C    3.870717   0.396592  -0.831777
C    4.961904   1.194313  -0.987884
C    6.182661  -0.139896   0.719803
H    5.099665  -1.755287   1.584110
H    2.964231   0.585675  -1.399248
H    4.981229   2.033690  -1.673525
H    7.087042  -0.308183   1.296601
N   -0.762081  -0.659926  -0.192326
C   -1.860683   0.044311   0.425171
C   -3.127549  -0.359071  -0.328051
O   -3.075185  -1.133865  -1.275783
H   -1.020320  -1.256793  -0.974225
H   -1.939771  -0.220433   1.485998
H   -1.709335   1.128615   0.367396
N   -4.271116   0.186915   0.117068
C   -5.532892  -0.119217  -0.516896
C   -6.619216   0.653502   0.194116
O   -6.420579   1.394496   1.125933
O   -7.818047   0.413659  -0.336873
H   -4.298481   0.827830   0.902803
H   -5.756124  -1.190620  -0.466659
H   -8.481304   0.928707   0.150064
H   -5.523995   0.157041  -1.576870
O    7.140689   1.738725  -0.413829
H    7.913194   1.536072   0.136286
```

TS_1b-2.xyz

34

C -3.837071 -1.410837 -0.304575
C -2.549194 -2.051243 0.038749
O -2.398911 -3.168646 0.449057
C -3.986843 -0.068440 -0.361094
C -2.922739 0.848859 0.007724
H -4.924745 0.350094 -0.718734
C -0.582335 2.344565 0.509102
C -1.901653 0.367794 0.942410
C -2.739133 2.077732 -0.620380
C -1.578450 2.808985 -0.406718
C -0.765438 1.177303 1.215510
H -2.254699 -0.261651 1.759999
H -3.481464 2.439614 -1.324994
H -1.419605 3.743194 -0.937670
H -0.060074 0.909465 1.994547
N -1.400475 -1.170901 -0.119488
C -0.085994 -1.691975 0.242538
C 0.924392 -0.809594 -0.497074
O 0.543792 -0.117543 -1.438057
H -1.321088 -0.720662 -1.045519
H 0.044891 -1.666493 1.328768
H -0.003584 -2.735145 -0.083672
N 2.187097 -0.858167 -0.065286
C 3.231108 -0.096800 -0.719226
C 4.523125 -0.348112 0.026866
O 4.605396 -1.068590 0.991255
O 5.536089 0.321565 -0.514870
H 2.476251 -1.438286 0.717171
H 3.002219 0.974083 -0.705384
H 6.346628 0.130158 -0.014949
H 3.346232 -0.394701 -1.766790
H -4.650604 -2.092897 -0.525674
O 0.524678 3.054786 0.748229
H 0.526291 3.904712 0.288430

TS_1b-7.xyz

34

```
C   -1.732957   -2.318755    0.177462
C   -0.914165   -1.089291    0.226697
C   -3.067642   -2.243872    0.007753
C   -3.766968   -0.973577    0.040788
H   -3.631491   -3.144779   -0.224320
C   -4.753543    1.653424   -0.074366
C   -3.258755    0.059597    0.930294
C   -4.816035   -0.677593   -0.830012
C   -5.295040    0.618211   -0.910620
C   -3.770199    1.374474    0.846051
H   -2.872109   -0.266994    1.891906
H   -5.212577   -1.446369   -1.485491
H   -6.080533    0.865351   -1.619727
H   -3.441487    2.145131    1.532603
H   -1.213276   -3.270958    0.161199
N    0.395565   -1.218432    0.127862
H    0.852217   -2.127450    0.030650
C    1.307438   -0.092238    0.110888
H    1.079384    0.570767   -0.730709
H    1.215011    0.487189    1.035545
C    2.713995   -0.682961   -0.026552
O    2.865247   -1.895302   -0.115710
N    3.719514    0.201169   -0.041149
H    3.568724    1.201597    0.041882
C    5.094387   -0.233121   -0.161200
C    5.974890    0.995418   -0.114519
H    5.369522   -0.911978    0.652970
H    5.263458   -0.768234   -1.101789
O    5.550407    2.119853   -0.000648
O    7.263166    0.677576   -0.213625
H    7.790417    1.492117   -0.175460
O   -1.425018    0.069489    0.309121
O   -5.230069    2.899382   -0.130773
H   -5.975119    2.989180   -0.739152


TS_2-3.xyz
  34


C    1.773805    2.770022    0.605306
C    0.895532    2.337496   -0.359617
O   -0.002370    3.126050   -0.965442
```

```
C    2.665995   1.852213   1.200121
C    2.678783   0.529933   0.794684
H    3.367412   2.192675   1.954396
C    2.972687  -2.007819  -0.440842
C    1.688654   0.040292  -0.153620
C    3.642135  -0.414922   1.270161
C    3.777918  -1.639207   0.690009
C    1.999523  -1.168159  -0.899740
H    0.675301  -0.425381   0.599745
H    4.307986  -0.112675   2.072681
H    4.530235  -2.334041   1.053845
H    1.407729  -1.483080  -1.751304
N    0.860836   1.045657  -0.815253
C   -0.402687   0.537433  -1.335408
C   -1.202173  -0.100988  -0.196946
O   -0.609497  -0.568520   0.809760
H    0.072371   4.038216  -0.654546
H   -0.965454   1.347594  -1.796368
H   -0.217344  -0.218189  -2.103236
N   -2.513894  -0.161121  -0.303381
C   -3.351791  -0.791940   0.703086
C   -4.791326  -0.605644   0.267764
O   -5.102548  -0.027414  -0.744264
O   -5.633396  -1.151816   1.134368
H   -3.006991   0.251960  -1.093380
H   -3.196186  -0.332192   1.683810
H   -6.545111  -1.014563   0.827131
H   -3.123195  -1.858503   0.793780
H    1.784745   3.819074   0.876868
O    3.156885  -3.182971  -1.079762
H    3.924985  -3.657535  -0.740012


TS_3-4.xyz
  34


C   -1.477717   2.890078  -0.456308
C   -0.393528   2.246815   0.055392
O    0.847016   2.736551   0.304030
C   -2.667377   2.190307  -0.714752
C   -2.706489   0.775807  -0.509609
H   -3.536558   2.705627  -1.102944
```

```
C   -2.685773   -2.029449   -0.159334
C   -1.587149    0.099337    0.011389
C   -3.827518   -0.017126   -0.833842
C   -3.826095   -1.388662   -0.664454
C   -1.560274   -1.276529    0.182221
H    0.679573    0.323110   -0.119675
H   -4.711358    0.472909   -1.230664
H   -4.705475   -1.970788   -0.924062
H   -0.699468   -1.802163    0.588596
N   -0.393074    0.848665    0.393946
C    0.090578    0.574481    1.797026
C    1.365255   -0.249367    1.641901
O    1.837939   -0.991029    2.444395
H    0.913941    3.673830    0.076706
H    0.316059    1.515993    2.303839
H   -0.652217    0.012398    2.364921
N    1.864845   -0.081632    0.279301
C    2.700706   -1.170341   -0.248536
C    3.870453   -0.538208   -0.978875
O    4.074523    0.651776   -0.969039
O    4.610531   -1.446317   -1.593635
H    2.394328    0.806512    0.189291
H    2.127600   -1.805857   -0.927303
H    5.364258   -1.014423   -2.029932
H    3.080427   -1.784091    0.575877
H   -1.396632    3.948517   -0.682823
O   -2.598954   -3.361647    0.026830
H   -3.415756   -3.808345   -0.228500


TS_3-5a.xyz
  34


C   -2.127850    2.811500    0.041800
C   -1.008038    2.147810   -0.439307
O    0.139062    2.697385   -0.850800
C   -3.229962    2.078226    0.447841
C   -3.230052    0.663094    0.326645
H   -4.113837    2.583964    0.821731
C   -3.154429   -2.119973   -0.088192
C   -2.076631    0.012235   -0.158146
C   -4.357102   -0.144172    0.610839
```

C -4.324470 -1.504087 0.411438

C -2.021373 -1.361732 -0.366034

H -0.231269 0.339400 -1.093459

H -5.259894 0.327803 0.986316

H -5.198463 -2.109737 0.632836

H -1.127299 -1.845081 -0.750049

N -0.896204 0.773166 -0.379552

C 0.456696 0.316229 0.915390

C 1.527109 -0.117409 -0.050019

O 1.200734 -0.428054 -1.206527

H 0.080566 3.661403 -0.901114

H 0.635937 1.214498 1.502820

H -0.058194 -0.487542 1.435749

N 2.786142 -0.144679 0.380513

C 3.872097 -0.564548 -0.483743

C 5.157833 -0.452001 0.306250

O 5.203777 -0.079412 1.453125

O 6.208653 -0.814304 -0.422122

H 3.036637 0.103773 1.333534

H 3.927716 0.065501 -1.377268

H 7.012393 -0.730099 0.116797

H 3.735657 -1.597811 -0.819729

H -2.130234 3.895734 0.066067

O -3.070014 -3.440480 -0.310611

H -3.899944 -3.893339 -0.114057

TS_4-6a.xyz

34

C 0.094498 3.065602 -0.237748

C 0.645117 2.210663 0.698194

O 1.767284 2.393684 1.401495

C -1.046809 2.679758 -0.939919

C -1.698268 1.452927 -0.664210

H -1.445669 3.331654 -1.710062

C -2.782490 -1.090723 0.001330

C -1.192162 0.690074 0.418820

C -2.776790 0.895294 -1.395956

C -3.271285 -0.378818 -1.082183

C -1.716033 -0.570939 0.814206

H -0.214118 -1.875990 -1.041624

```
H   -3.197309   1.451145  -2.226302
H   -4.084317  -0.793904  -1.671931
H   -1.745280  -0.854750   1.864692
N    0.013170   1.031049   0.978574
C    0.643971  -0.059949   1.694497
C    0.249059  -1.369415   0.960377
O    0.412039  -2.467806   1.418745
H    2.248289   3.172222   1.091838
H    1.723521   0.092835   1.737078
H    0.251181  -0.178726   2.708772
N    0.550987  -1.322732  -0.644713
C    1.863146  -1.916109  -0.987731
C    2.904417  -0.819599  -0.899464
O    2.617570   0.334311  -0.673983
O    4.121370  -1.286182  -1.113055
H    0.493045  -0.366530  -1.015191
H    1.850025  -2.325986  -2.001029
H    4.768441  -0.561796  -1.073050
H    2.073337  -2.726579  -0.283083
H    0.575112   4.017532  -0.432827
O   -3.255593  -2.289859   0.407069
H   -4.044950  -2.545114  -0.087744
```

TS_7-6b.xyz

```
 34

C    2.259979  -1.916313   0.854434
C    2.231819  -1.216300  -0.327590
C    1.051555  -2.425184   1.375815
C   -0.152403  -2.030608   0.794433
H    1.051767  -3.032808   2.274214
C   -2.494282  -1.314219  -0.649603
C   -0.103401  -1.179212  -0.374554
C   -1.444802  -2.360934   1.289721
C   -2.573361  -2.001147   0.603300
C   -1.271469  -0.975035  -1.174952
H    0.094124   0.179223   0.027616
H   -1.523528  -2.937021   2.206688
H   -3.551097  -2.270847   0.994488
H   -1.200771  -0.484255  -2.140436
H    3.191067  -1.994242   1.403238
```

```
N    3.225783  -0.451828  -0.871230
H    4.096452  -0.480572  -0.352923
C    2.793397   0.906169  -1.246075
H    3.682645   1.510934  -1.424617
H    2.193736   0.865736  -2.156352
C    2.031476   1.516706  -0.063786
O    2.567142   1.896369   0.941342
N    0.587323   1.447658  -0.121695
H    0.209957   1.646658  -1.058049
C   -0.130496   2.251718   0.884730
C   -1.490578   2.585129   0.303328
H   -0.233001   1.689620   1.816482
H    0.417984   3.170919   1.111788
O   -1.786179   2.349647  -0.843987
O   -2.276606   3.164566   1.198112
H   -3.121865   3.401801   0.780720
O    1.110531  -1.151659  -1.087618
O   -3.596136  -0.996103  -1.354663
H   -4.393831  -1.383123  -0.973059
```

```
TS_7-8.xyz
  34

C   -1.477704  -2.531918   0.997199
C   -0.917776  -2.196381  -0.209882
C   -2.498189  -1.700940   1.517706
C   -2.718667  -0.463158   0.916684
H   -3.012329  -1.965238   2.435257
C   -3.117926   1.953120  -0.530210
C   -1.961168  -0.145758  -0.280306
C   -3.570278   0.556735   1.424447
C   -3.748138   1.726086   0.735234
C   -2.302576   0.994164  -1.075941
H   -0.677694   0.192698   0.112505
H   -4.101369   0.385170   2.355653
H   -4.405453   2.492391   1.138456
H   -1.857276   1.134566  -2.055176
H   -1.064523  -3.350081   1.575559
N    0.245282  -2.663382  -0.755937
H    0.724120  -3.368769  -0.210314
C    1.095017  -1.657982  -1.382936
```

```
H     2.009855   -2.145580   -1.722286
H     0.589420   -1.246636   -2.259953
C     1.444398   -0.490234   -0.447543
O     0.601199    0.196191    0.198809
N     2.723331   -0.188389   -0.325430
H     3.449066   -0.718110   -0.804754
C     3.197198    0.921054    0.483759
C     4.708600    0.943570    0.371869
H     2.780641    1.869509    0.130607
H     2.901014    0.796294    1.529942
O     5.330904    0.146324   -0.285806
O     5.231776    1.935196    1.079794
H     6.198993    1.923134    0.985037
O    -1.484745   -1.259708   -1.008055
O    -3.321316    3.088707   -1.229227
H    -3.974048    3.659210   -0.805580
```

TS_8-5b.xyz

```
  34

C     1.765012   -2.420435   -0.201748
C     1.035715   -1.263314   -0.517664
C     3.091705   -2.292315    0.118089
C     3.699664   -0.999963    0.147529
H     3.689854   -3.168906    0.345059
C     4.738541    1.605755    0.163521
C     2.904261    0.124473   -0.147705
C     5.054351   -0.768939    0.454334
C     5.571477    0.509634    0.464702
C     3.389836    1.416268   -0.146188
H    -0.674059   -0.429163   -1.314381
H     5.692964   -1.615727    0.686263
H     6.617687    0.676559    0.702268
H     2.754270    2.261130   -0.383473
H     1.271156   -3.384507   -0.242048
N    -0.304370   -1.218200   -0.740087
H    -0.713141   -2.111573   -1.003036
C    -1.450144   -0.576289    0.735500
H    -1.703120   -1.438986    1.346498
H    -0.727068    0.112941    1.162820
C    -2.502998    0.056806   -0.116962
```

O	-2.178536	0.563717	-1.198558
N	-3.768501	0.014096	0.317438
H	-4.017341	-0.369159	1.224369
C	-4.841812	0.621755	-0.441199
C	-6.125684	0.425110	0.334161
H	-4.665481	1.691956	-0.594502
H	-4.934552	0.164124	-1.431560
O	-6.181487	-0.132678	1.402958
O	-7.167489	0.943312	-0.309640
H	-7.968447	0.802947	0.221458
O	1.571480	-0.036357	-0.451442
O	5.179590	2.871672	0.155431
H	6.119381	2.928497	0.370584